CHALMERS
UNIVERSITY OF TECHNOLOGY

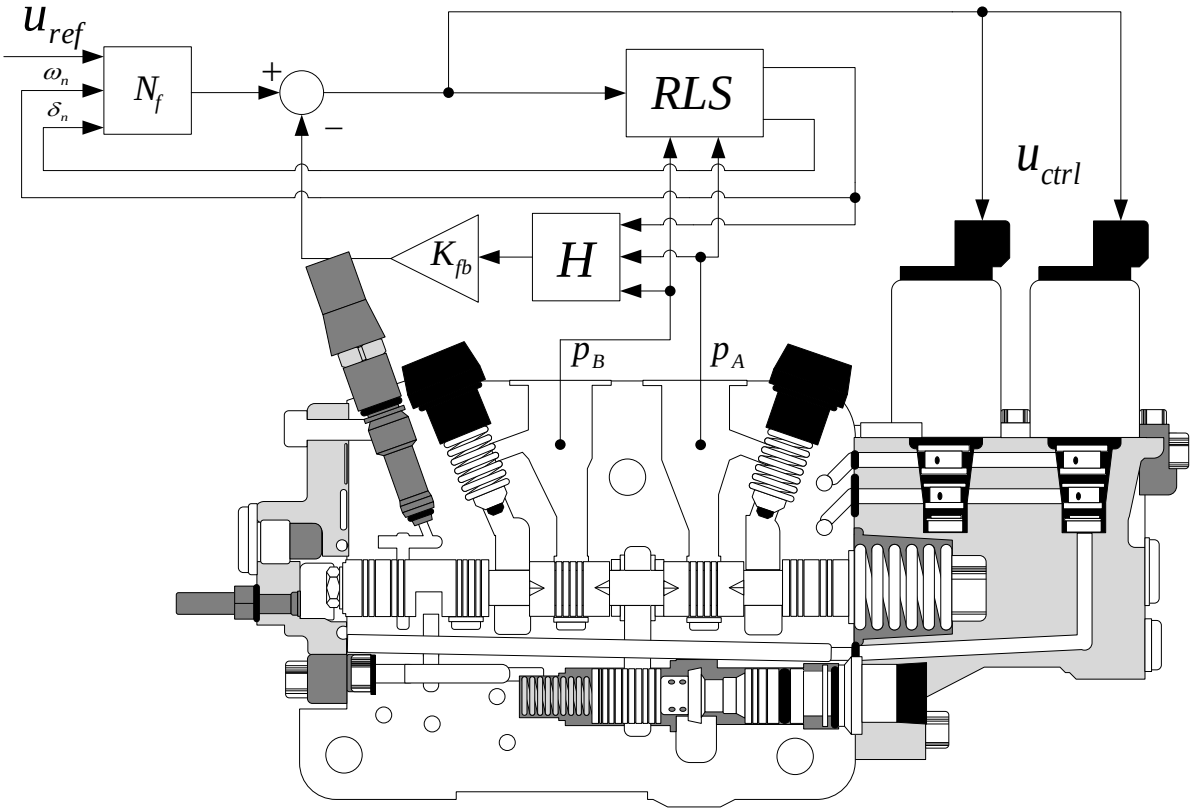

Embedded Implementation of Active Damping in Hydraulic Valves

An Adaptive Control Solution

Master's thesis in Systems, Control and Mechatronics

MARCUS MÅRLIND

Department of Electrical Engineering
CHALMERS UNIVERSITY OF TECHNOLOGY
Gothenburg, Sweden 2017

Master's thesis 2017:41

Embedded Implementation of Active Damping in Hydraulic Valves

An Adaptive Control Solution

MARCUS MÅRLIND

CHALMERS
UNIVERSITY OF TECHNOLOGY

Department of Electrical Engineering
Division of Systems and Control
Chalmers University of Technology
Gothenburg, Sweden 2017

Embedded Implementation of Active Damping in Hydraulic Valves
An Adaptive Control Solution
MARCUS MÅRLIND

Supervisor: Hans Bodén, Parker Hannifin AB
Johan Hansson, Parker Hannifin AB
Johan Magnusson, Parker Hannifin AB
Examiner: Bo Egardt, Department of Electrical Engineering

Master's Thesis 2017:41
Department of Electrical Engineering
Division of Systems and Control
Chalmers University of Technology
SE-412 96 Gothenburg
Telephone +46 31 772 1000

Cover: Graphical illustration of a cross section view from an L90LS valve, displaying its different components and a simplified block diagram of the adaptive control solution.

Gothenburg, Sweden 2017

> It is not knowledge, but the act of learning, not possession but the act of getting there, which grants the greatest enjoyment.
>
> — *Carl Friedrich Gauss (1777 - 1855)*

Embedded Implementation of Active Damping in Hydraulic Valves
An Adaptive Control Solution
MARCUS MÅRLIND
Department of Electrical Engineering
Chalmers University of Technology

Abstract

The objective of this thesis is to implement an embedded solution of active damping in hydraulic valves, which aims at reducing vibrations in mobile machines with on-board electronics. Oscillations in mobile machines are usually problematic and have been for a long time. They often occur due to the fast movements with requirements of heavy loads. The solutions are often in form of limiting the operator's speed of using built-in damping in the valve. However, these solutions have often drawbacks in form of decreased efficiency and moderate damping effect. With the developments in electrification in hydraulics it is now more convenient to use control strategies to reduce oscillations and vibrations with software.

Active damping has previously been done but experiments with embedded implementations needs to be investigated further. This thesis derives an adaptive control solution which is based on different papers and previous master's thesis projects, and implements it on a mobile machine, a forwarder.

The main conclusion that can be drawn from this thesis is that the embedded processor, with fixed-point arithmetic, is not sufficient for the derived algorithms to be fully adaptive to system changes. Instead a simpler method has been used for the experiments in laboratory environment and on the forwarder. The experiments indicate that the simpler method for the active damping solution will still dampen the system drastically, and approximately reduce pressure oscillations by 30-50%.

Keywords: Adaptive control, MATLAB/Simulink, active damping, hydraulic valves, recursive least square, identification, embedded systems.

Acknowledgements

I would like to take this moment to express my gratitude to Parker Hannifin AB in Borås for letting me do this master's thesis, and a special thanks to Hans Bodén. I would also like to thank my supervisors, Johan Hansson and Johan Magnusson, for the contribution, interest, and constant support in my work, which has helped me a lot in the learning process during these couple of months.

Special thanks to Jonas Hjälte, for his view and explanation of hydraulic systems, Ulf Nyberg, for his help and support with the electronic hardware setups, and to everyone else that in some way have supported or showing interest in my master's thesis.

Finally, I would like to thank my family for encouraging me during my entire educational life, and most of all my girlfriend Emma, for always being supportive and helping me put together the final pieces of this master's thesis.

Marcus Mårlind, Gothenburg, June 2017

Contents

List of Figures

List of Tables

Nomenclature

Symbol	Description	Units
β	Bulk modulus	Pa
δ_n	Estimated damping for the system	–
δ_v	Damping ratio for the valve	–
Δp	Pressure difference	Pa
ΔV	Volume difference	m^3
$\Gamma(t)$	The trace of the covariance	–
γ_{max}	The maximum covariance of $P(t)$	–
$\hat{\theta}(t)$	Estimated parameters for the RLS algorithm	–
$\lambda(t)$	Varying forgetting factor	–
λ_0	Initial value of the forgetting factor	–
ω_a	Continuous analogue frequency	rad/s
ω_d	Modified frequency	rad/s
ω_n	Estimated resonance frequency	rad/s
ω_v	Resonance frequency for the valve	rad/s
ω_{bh}	Higher break frequency	rad/s
ω_{bl}	Lower break frequency	rad/s
$\theta(t)$	True parameters for the RLS algorithm	–
$\varepsilon(t)$	Parameter prediction error	–
$\varphi(t)$	Regression vector	–
ξ_1	Width of the notch filter	–
ξ_2	Depth of the notch filter	–
$a(t)$	Variable for turning on and of the RLS	–
A_1	Area of chamber 1	m^2
A_2	Area of chamber 2	m^2
B	Damping friction	Ns/m
B_p	Friction coefficients in the cylinder	Ns/m
$B_{p3}(s)$	Third order band-pass filter	–
C_1	Capacitance in chamber 1	m^5/N
C_2	Capacitance in chamber 2	m^5/N
C_{Le}	The effective capacitance	m^5/N
d	Cylinder diameter	m
d_2	Piston diameter	m
f	Load disturbance	N

$G_1(s)$	Transfer function from piston position to load pressure	–
$G_2(s)$	Transfer function from spool position to load pressure	–
$G_v(s)$	Transfer function from input signal to spool position	–
$G_{fxp}(s)$	Transfer function from load force to spool position	–
$G_{pxp}(s)$	Transfer function from load pressure to piston position	–
$G_{up}(s)$	Transfer function from input signal to effective load pressure	–
$H(s)$	Transfer function of the dynamic pressure feedback filter	–
$H_2(s)$	Second order high-pass filter	–
$K(t)$	The correction gain vector	–
K	Stiffness	N/m
K_c	Flow-pressure coefficient	m^5/N
K_q	Flow gain	m^2/s
K_{fb}	Feedback gain for the dynamic pressure feedback	–
l	Piston length	m
M_1	Mass of the crane base	kg
M_2	Mass of the cranes arm	kg
$N_f(s)$	Transfer function of the notch filter	–
$P(t)$	Covariance matrix	–
p_1	Pressure in chamber 1	Pa
p_2	Pressure in chamber 2	Pa
p_{Le}	Effective load pressure	Pa
q	Oil flow	m/s
T	Sampling time	s
$V_N(\theta)$	Quadratic cost function	–
x_C	Cylinder position	m
x_L	Load position	m
x_P	Piston position	m

Chapter 1

Introduction

1.1 Background

The use of hydraulic valves can be found almost anywhere in an industrial application or process. They are included in process industries, mining, processing of oil, in machinery, material handling, forestry and in many other fields. This makes the performance and functionality of a hydraulic valve important to investigate, and to improve.

Today, there are problems with disturbances, such as vibration and oscillations, in many applications. In hydromechanical systems, especially mobile machines, such as cranes, forestry machines, wheel loaders, and excavators, oscillations can influence the performance and the controllability of the machine. The two main reasons why oscillations occur in these systems are:

- The compressibility of the fluid in the hydraulic valves.
- The flexibility of the mechanical structure.

The mobile machines mentioned above are supposed to bear large loads, and this creates high pressure in the hydraulic systems, tending to create oscillations. Mobile machines are often weaker than stationary systems making them more flexible. The combination of a light construction and high pressure in the hydraulics systems, tend to cause severe problems with oscillations.

In most mobile machines, there is an operator who controls the machine's movements and functions. The hydraulic valves transfer those movements to the various parts of the machine, for instance to a crane's arm on a forwarder. If such systems are influenced by oscillations it could cause an unpleasant behaviour for the operator when in use. The machine becomes less smooth, causing the operator to be much more careful when controlling the machine. The oscillations can occur when the operator controls the hydromechanical system at its resonance frequency. It could also occur from sudden load disturbances.

Today's solutions are often done by dampening/soften movements by passive damping. In recent years more interest has been in solutions where active

damping is implemented instead, which implies that the hydraulic actuators are controlled in a certain way to avoid unnecessary oscillations.

The method of using active damping has previously been done on hydraulic valves with a method called CADO, which stands for "Controller for Active Damping of Oscillations", in [20]. This method has been validated through simulations and in experiments, but embedded tests and evaluations on real applications have not been carried out extensively.

The focus of this master's thesis will be to investigate an embedded control implementation of active damping in valves, and to improve what has previously been done within this field. The project will be done with the help of the company Parker Hannifin located in Sweden, Borås, where experiments can be done at their test site and with the right equipment.

1.2 Aim

The aim of this thesis is:

- To implement active damping for an embedded application in hydraulic valves to be used in mobile machines.
- Evaluate different algorithms that are used in the active damping solution.
- To evaluate the performance of the solution and analyze its limitations.

1.3 Problem formulation

The focus of this thesis is to reduce the oscillations on mobile machines by only controlling the hydraulic valves. This implies that the controlling and measuring can only be done from the valve, i.e. controlling the actuators and measuring pressure changes.

When an oscillation is affecting a hydromechanical system, the same oscillation will also appear in the pressure. Therefore, the main goal is to create a control algorithm which dampens the oscillations in the pressure difference between the valve and the hydraulic cylinder, which actuates the functions to the hydromechanical system. This can be achieved by identifying the resonance frequency that causes the most critical oscillations, and dampen it. The identification combined with some filter design can significantly reduce the oscillations on these types of systems [20].

In order to accomplish this, the task is split into the following steps:

1. Create a mathematical model of a hydromechanical system.
2. Create an adaptive control algorithm that dampens the vibrations on the mathematical model in Simulink.
3. Generate code for the embedded application from the Simulink model.

4. Construct a CAN system in order to communicate with the devices, which allow control of the input- and output signals to the system.
5. Import the generated code into Parker Hannifins electrical control unit, CM2620 [14].
6. Test the derived control algorithm in a closed lab environment and tune the different parameters.
7. Validate the active damping solution on a mobile machine.

1.3.1 Research questions

In relation to the problem formulation some research questions were generated in the beginning of the project. These are listed below:

RQ-1: What types of models are needed for testing and validating a control strategy?

RQ-2: For a hydraulic valve system, what control strategies are suitable to use?

RQ-3: How can robustness be achieved by applying active damping to different hydraulic systems?

This thesis intends to answer these questions by firstly conduct a literature study and by implementing practical solutions.

1.4 Scope and boundaries

The scope of this master's thesis is to focus on the embedded implementation of active damping. For the implementation to be possible the following four statements need to be fulfilled:

(i) The resonance frequency of the mechanical structure is identified or approximately chosen.

(ii) The pressure difference from the valve to the hydraulic cylinder can be measured.

(iii) The control unit has enough RAM and the processor needs to be able to do all the necessary calculations with sufficient resolution.

If all of these statements are satisfied then the active damping method can be implemented on an embedded processor.

1.5 Problem Discussion

This section will go through why this problem is necessary to investigate, and current solutions that exist today.

1.5.1 The benefits of a system free from oscillations

Benefits of a system free from oscillations can be summarized into two sections, operator aspects and sustainability aspects.

1.5.1.1 Operator aspects

Reducing oscillations by active damping can be beneficial to those who are operating the machines. A person that must spend most of his/her day in a vibrating machine may experience increased stress levels, vertigo, or muscle ache. Reducing the oscillations can therefore create a safer work environment. This can also increase the operator's ability to smoothly maneuver the machine. A less vibrating machine will decrease the risk of damaging the machine itself and objects in its environment and also increase the productivity. Knowing that the machine is well damped may lead to greater control of the machine, making the operator steer as fast as he/she desires. This is one of the most crucial factors to a crane operator. If the operator feels restricted by new functions, in terms of lack of ability to operate at a desired speed, they may tend to turn off that function, creating an unsafe work environment.

Recently more focus has been put to designing smoother control for the operators, which often results in reduced performance of the machine. This creates a trade-off between smooth control and performance.

This is the main outcome for the operator of an oscillation free system, increased health and facilitated workload, making it easier for new crane operators to learn the machine while increasing the productivity.

1.5.1.2 Sustainability aspects

If the vibrations are reduced or removed, the machine could become more easily controlled, making it need less correction and therefore demanding less energy. The reduction of vibrations can also increase the life time of the systems parts, saving investment and maintenance cost. There is currently an interest in reducing the energy cost of the distinct functions in mobile machines by using software, and the suggested solution in this thesis could come to be a useful asset for that mission.

1.5.2 Current solution

One of the current solutions to the oscillation problem is to ramp the control signals. This means that the acceleration and deceleration of the mobile machine will be limited, decreasing the work speed and the efficiency and therefore, limiting the operator's control capabilities. This solution does prevent the occurrence of oscillations to a certain degree but creates a slower system response, which is not desirable.

Current industrial practices uses basic control theory, such as PI-regulators and logic, for controlling individual functions. This has been shown to give acceptable results, however, it is very time consuming to find a good set of

parameters for a given function on a given machine. Therefore, this method is not applicable in this situation.

At Parker Hannifin, the development of control structures for mobile machines are done within their IQAN software, which allows for easy communications and control of different functions. However, it is very limiting regarding customization of algorithms, and on applied control theories. These algorithms currently need to be executed on a separate control unit, which allows more freedom and bypassing the IQAN system.

1.5.3 Previous work in adaptive control in hydraulic valves

In, [20] active damping was used, but the experimental tests were carried out with a computer using floating point arithmetic, and without any major restrictions for the algorithm. The work in adaptive control in hydraulic valves were developed during the 90's by Svante Gunnarsson and Petter Krus at Linköpings University. They investigated how recursive identifiers and filter could be used in order to control valves, e.g. [6], [7]. Their work was also used in [20] and in this thesis. These methods were implemented and tested in experiments, however they are not as often seen in the industry today. Since the development of hydroelectric control have increased for mobile systems, hydraulic companies are now more interested in these types of techniques, and how they can be implemented.

Considering the above, there is an interest in investigating how well a solution of active damping can work with the on-board electronics that is available today. Therefore, there is a limit on how fast the algorithm can be and how much RAM it can take up in the given processor.

Depending on how well the algorithm can be adapted to the given system, development cost and time may vary and therefore, the limitations, and how they can be overcome, is discussed in this master's thesis.

1.6 Schematic view of the hydraulic system

In this thesis, the hydraulic system that the active damping should operate on can be seen in the following Figure 1.1.

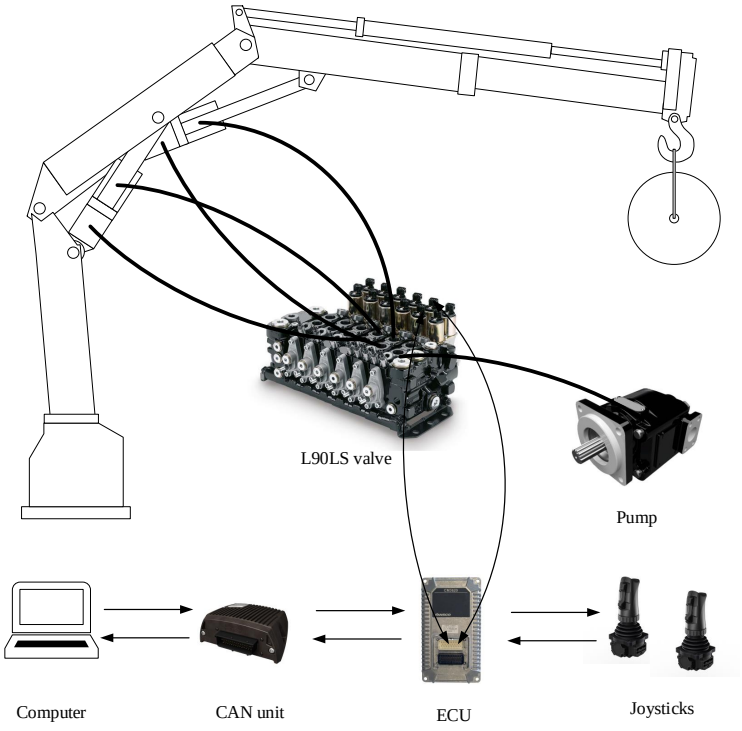

Figure 1.1: A schematic view of the hydraulic system used in this project, where the crane is based from [8] and the components images from [12], [14], [13], [10], [11].

The hydraulic system is controlled from joystick input, which control the flow and pressure in the valves, which then control the different functions on the crane. The active damping is implemented as embedded code which is executed on the electrical control unit (ECU). The ECU is connected to a CAN network with a CAN unit for easy access of system parameters and logging of data on a computer. In this thesis, everything from creating the embedded code, reading the pressure measurements, reading the joysticks inputs, and creating the CAN network has to be done. This means that the adaptive solution will bypass any other software that is already created for Parker Hannifin's current control system. The suggested solution in this thesis will not be a software that is ready to launch, instead it will point in a direction of how adaptive control solutions can be implemented in hydraulic systems.

Chapter 2

Valve Theory

In order to understand why oscillations occur in hydraulic valves, the basic valve theory will be explained. This chapter will go through different characteristics of valves and how they function. Explanations of the valve that will be used in the experiments are also included.

2.1 Valve characteristics

When it comes to hydromechanical systems there are several diverse types of valves on the market, depending on what type of function and behaviour that is needed. The flow characteristics of a valve can be related to the type of valve center [17]. There are three main types of valve centers that exists, closed center, critical center, and open center valve. They differ in how the spool inside the valve moves and in what way it allows the fluid to move to the different service ports.

The most important characteristic of a valve is the flow gain and this can be described by a relationship between the load flow and the spool stroke. This is instructed in Figure 2.1 for different types of valve centers.

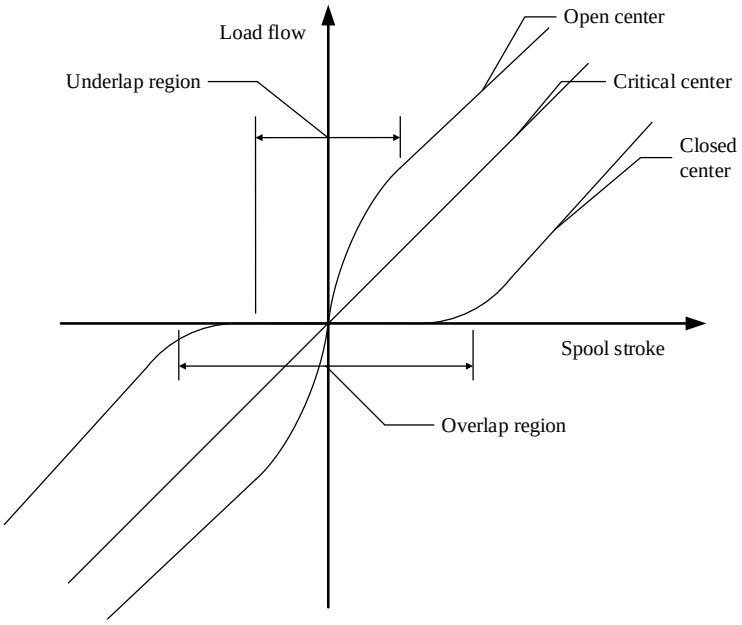

Figure 2.1: The flow characteristics for the three types of valve centers, open, closed, and critical [17].

The figure displays how the flow from the valve will behave for a given spool stroke, also called spool displacement. The relationship between load flow and spool stroke in a valve is a nonlinear behavior. The critical center valve in Figure 2.1 is used to describe the ideal linear behavior of a valve. Open center means that the spool is always open in neutral spool position, and are used when it is required to have a continuous flow for different fluid temperatures. This means that the open center valve has a constant flow from the pump. The main advantage is that it has high damping and is simple to use and design. However, one of its major drawbacks is that it has some severe problems with accuracy of positioning heavy loads, which is often done with cranes [2]. Closed center valves are always closed in neutral spool position and are energy efficient, but it has dead-band characteristics creating a slow response [17], which can be seen be the overlap region in Figure 2.1. Since an open center valve always has continuous pump flow, the valve is constantly draining energy from the system, even if a hydraulic function is in a fixed position. In a closed-center valve the pump flow is variable with load sense, reducing energy waste when a hydraulic function is in a fixed position.

There are of course trade-offs when choosing which type of valve that should actuate the hydraulic function. For example, the open-center valve is commonly preferred by operators, since it allows some steering feedback on the controller joysticks. But from an energy saving perspective, the closed-center valve is commonly used in the industry, but they have a higher cost due to

their complex mechanical design.

2.1.1 Bulk modulus

One of the main reasons why oscillations occur is the compressibility of the fluid in the hydraulic valve. The compressibilty is dependent on the pressure difference ΔP and the volume difference ΔV [17]. The relation between the pressure and volume difference can then be described as a constant according to the equation

$$\beta = V\frac{-\Delta p}{\Delta V} \tag{2.1}$$

This constant is called the bulk modulus, and it is commonly around 1.5 GPa for fluids in hydromechanical systems.

2.1.2 Valve control

Depending on how and where the valve should operate, different control mechanisms exist. The most common way to control a hydraulic valve is by using a lever connected to the spool; the spool position then decides how much flow that is allowed to enter the specific port. Other ways are to use a pressure control or electric control, where the latter will be used in this thesis when carrying out the experiments. The benefits of using electric control valves is that control algorithms, and other techniques, can be applied to the system, given that the system has an electrical control unit (ECU); the drawback is that it can be expensive to install in some machines.

2.1.3 Spool properties and notations

Figures of spool notations are commonly used in the industry in order to easily see the properties of the spool. Different spools will give different performance of the valve, and they are usually manufactured with high tolerances due to sensitive mechanical characteristics. The following Figure 2.2 displays the notation used to represents a 4 ways 3 position spool that is commonly used in L90LS valves. Note that different spools can be used depending on what functions of the valve that is desired. There are for instance spools that have hydraulic pressure feedback, which is used as a passive damping property for the valve.

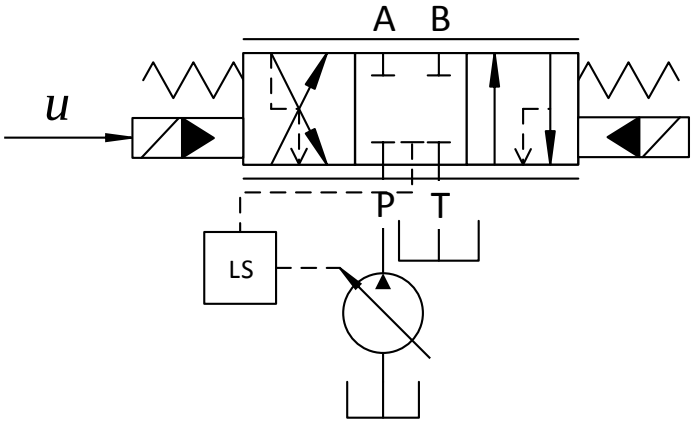

Figure 2.2: Figure of the spool used in the L90LS valve where P is the pump pressure, T represents the tank, u is the applied current for controlling the valve, A and B are the pressures from the respective chambers in the hydraulic cylinder. LS means that it has load sensing.

The above figure tells us how the pressure will be applied from the pump to the respective service port A or B, depending on how the spool moves. When the spool moves to the right, the left arrow box tells us that flow of the fluid will go from the pump to service port B and the flow in service port A will go to the tank. If the spool moves in the other direction the flow will be reversed, which is told by the right arrow box. This description means that the spool is double acting, e.g. used in double acting cylinders. The black triangle and the slash in the box right to u represent that the spool is electrically controlled with hydraulic pilot, and the spring symbol represents that is has a spring return of the spool [25]. The box with LS stands for load sensing and means that the spool can be compensated with a pressure level when a load is applied.

2.2 The L90LS valve

In this thesis, the L90LS valve from Parker Hannifin has been used [11]. The L90LS valve is a direction valve, which means that it allows fluid to flow in different directions from one or more sources. The L90LS valve consists of a spool that is inside a cylinder that can be mechanically or electrically controlled with magnetic/solenoid actuators from 12 V or 24 V. The solenoid then controls a flow to the spool, which is called the pilot pressure, it is this pressure that moves the spool.

The benefits from this valve is that it is pressure compensated which means that there is a constant pressure-differential between the pump and the service-port sides of the spool, resulting in a constant flow for any given

lever stroke [11]. This also means that it can hold the pressure if a load is suddenly dropped. Therefore, pressure compensators are usually used in forestry machines where good handling is desired [3]. The L90LS has a load sensing (LS) system which means that pressure and flow are modulated to match the immediate need of a pressure level to the heaviest load at the moment. This also improves the energy efficiency [3]. When it comes to the valve characteristics of the L90LS it has a closed center valve, which means it will have a dead-band behaviour of the flow. This will be needed to be compensated for, more on this in the embedded implementation in Chapter 6. The reason for the dead-band behaviour is that closed center valves are always closed in neutral spool position, which means that the spool will have a distance to travel before it starts to let flow pass through. For illustrative purpose the following Figure 2.3 displays where the dead-band occurs in a closed center valve.

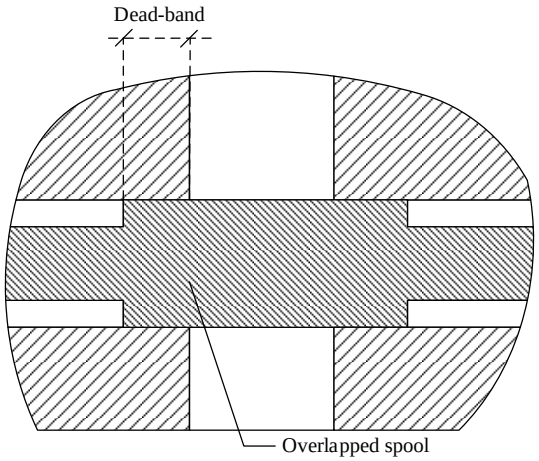

Figure 2.3: Cross section view displaying the dead-band effect from closed center valves.

The main reason to implement active damping on the L90LS valve is that it has good characteristics and it has been used in the industry for a long time, meaning that is a robust valve to use for electrical control. The most recent interest in the L90LS valve is to develop more on-board electronics which can increase the performance of the desired functions, and furthermore increase the flexibility and control for the operator.

2.2.1 Schematic view of the L90LS

In order to get a better understanding of the L90LS valve a cross section view is shown in Figure 2.4 displaying some of its major components.

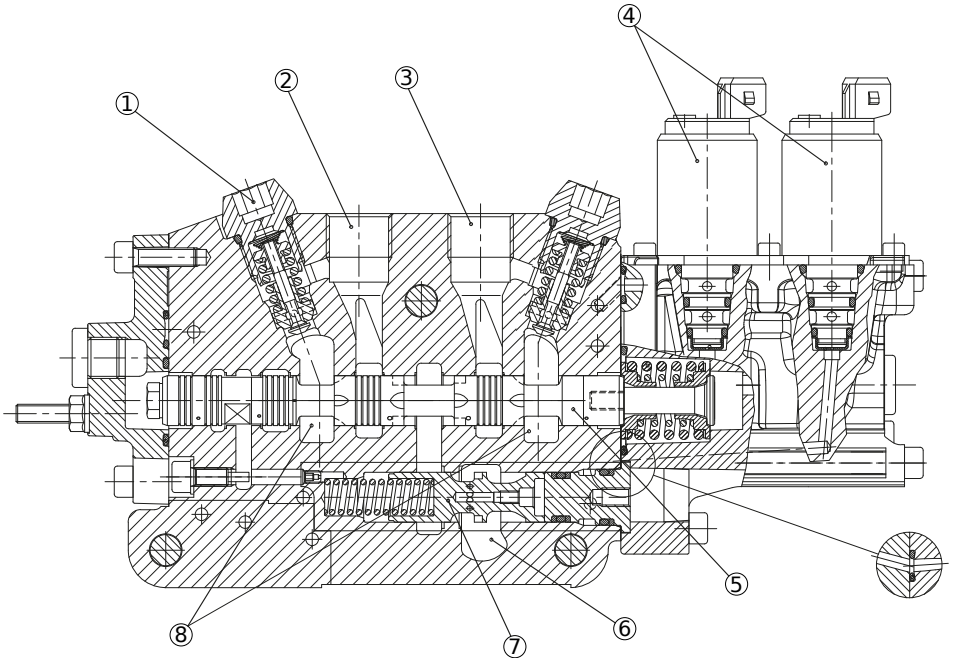

Figure 2.4: Cross section view of the L90LS valve showing its different components [15]

From the cross section view the two solenoids can be seen at (4). The L90LS has port relief valves that will open if the pressure gets too high, seen at (1). The ports that are connected to the cylinder are shown at (2) for port A and at (3) for port B. The pump is connected at (6) and the tank/reservoir at (8). Finally, the pressure compensator that was discussed previously is shown at (7). The most crucial parts for this master's thesis lies in controlling the two solenoids and measuring the pressure at port A and B, and therefore the other components will not be considered in the active damping.

Chapter 3

Mathematical Model

In this chapter, the mathematical models and their equations will be presented in order for the reader to fully understand how to simulate and control the behaviour of oscillations in hydraulic valves.

3.1 Mathematical model of a crane

In order to simulate and test different approaches for an active damping implementation, a mathematical model is needed. The model that will be used in this thesis is of a hydraulic crane, which has previously been derived in [9]. The main reason why the crane is such a good example to use is because it involves many functions which combine hydraulic cylinders actuated by valves. For instance, a crane can turn its arm, normally called the swing function, it can raise and lower its arm, called the boom function and it can tilt the end of the arm, which is called the jib function. The crane can be found on many mobile applications like forestry machines and excavators. This makes the modeling of a crane complex since it depends on what type of machine it is mounted on. It will also depend on the load and the environment. Therefore, the model derived in this thesis will be simplified.

For a better understanding of the derived equations, a detailed explanation of the model will be carried out. The first model of the crane will be of a boom function and then some simplifications can be done in order to describe it as the swing function. The following Figure 3.1 displays the crane's boom function and the hydraulics connected to it.

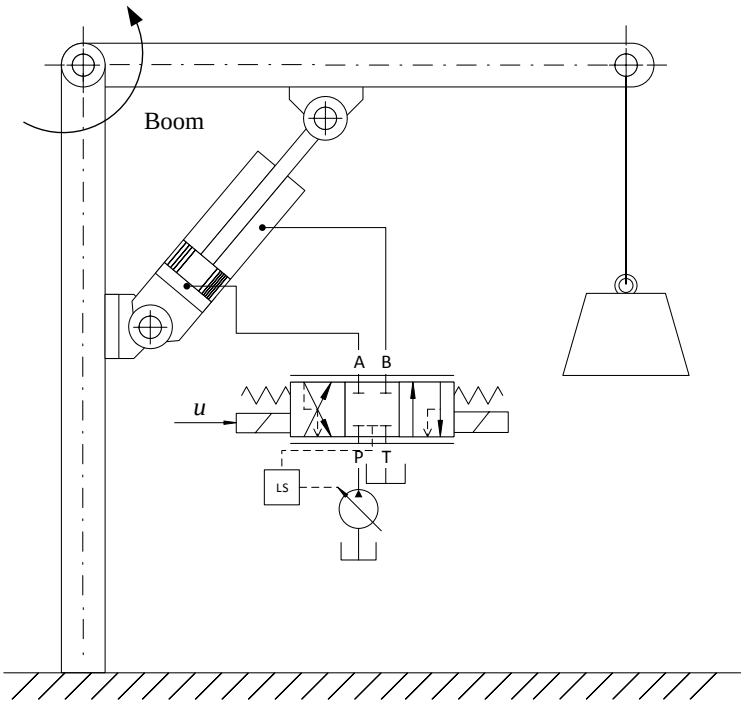

Figure 3.1: An overview of how a hydromechanical system could look like. Here a crane's boom function is presented, which has a valve that actuates the hydraulic cylinder and moves the arm up and down.

The system presented in Figure 3.1 has two outputs, piston position $x_p(t)$, and effective load pressure $p_{Le}(t)$, which is the pressure difference in the cylinder. The input will be a signal from -100% to 100% from the joysticks, which is then translated to a current reference input to the valve which then controls the flow to each function that the crane has. The crane presented above has two functions, swing and boom. For now, the boom function is only considered, which enables the arm of the crane to tilt upwards and downwards.

The crane can be seen as two masses where the flexibility is connected to the base of the crane, shown in Figure 3.2. In a mobile machine the flexibility can be seen a spring/damper system between the wheels and the surface.

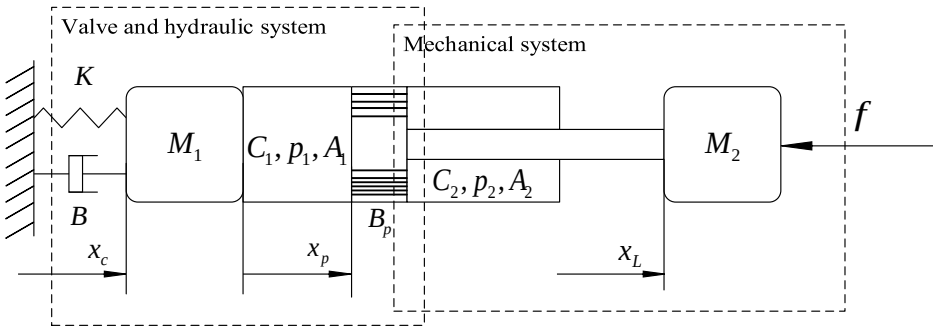

Figure 3.2: The crane model described as two masses where the flexibility is in the base of the crane [9].

By using force balance from the Figure 3.2 the following equations are obtained:

$$M_1\ddot{x}_c = -Kx_c - B\dot{x}_c + B_p\dot{x}_p - A_1p_1 + A_2p_2 \tag{3.1}$$

$$M_2\ddot{x}_L = -B_p\dot{x}_p + A_1p_1 - A_2p_2 - f \tag{3.2}$$

Here M_1 and M_2 are the masses, K is the spring stiffness, B is the damping friction, B_p a friction coefficient between the cylinder and the piston, A_1 is the cross-section area of chamber one, A_2 is the cross section area of chamber two, p_1 and p_2 are the pressure in their corresponding chambers, and f is the load disturbance. The arrows in the figure represent the cylinder position x_c, piston position x_p, and load position x_L.

One major simplification for this model is that the gravity and the length of the crane arm is not included in the model. Which means that the model will not show what happens if the angle of the crane is changed. This is not the case when looking at the swing function which does not depend on the crane's length, and gravity in the same way. The swing function will be presented in Section 3.4.

3.1.1 Oil characteristics

The mathematical models of oil volumes in a cylinder are described by a mass balance, such as

$$q\rho = \frac{d}{dt}(V\rho) \tag{3.3}$$

where q is the flow, ρ the density of the oil and V the volume. This equation then needs to be linearized around an operating point as in [17], which gives the following equations for the flow in chamber one and two from Figure 3.2

$$q_1 = A_1\dot{x}_p + C_1\dot{p}_1 \tag{3.4}$$

$$q_2 = A_2\dot{x}_p - C_2\dot{p}_2 \tag{3.5}$$

where $\dot{x}_p$ is the piston velocity, $\dot{p}$ is the pressure change, C_1 and C_2 are the capacitance for the two chambers, given by the relation

$$C_1 = \frac{A_1 l}{2\beta} \quad C_2 = \frac{A_2 l}{2\beta} \tag{3.6}$$

where l is the nominal chamber length, A_1 and A_2 are the area of the respective chambers, and β is the bulk modulus of the oil given in Equation (2.1).

3.1.2 Valve dynamics

The valve dynamics is important to include in the model since it describes how the flow will behave depending on the spool position and the pressure difference. The oil through a valve can be described by the equation

$$q = C_q d \pi x_v \sqrt{\frac{1}{2\rho} \Delta p} \tag{3.7}$$

where C_q and d are geometry parameters, x_v is the valve opening, and Δp the pressure difference. The following Figure 3.3 shows the basic concept of a valve opening. Note that the L90LS valve uses a spool that regulates the opening but for an easier interpretation this concept is used by a valve element that opens and closes on the valve base.

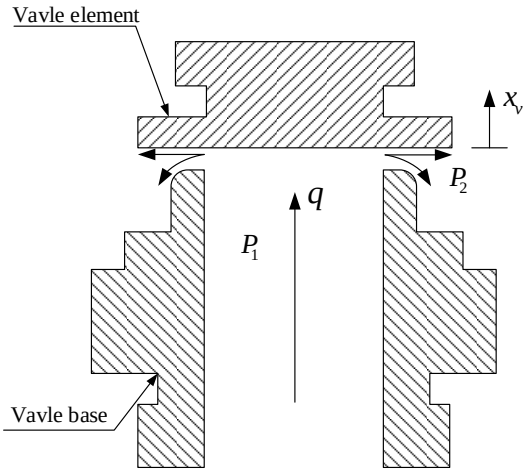

Figure 3.3: Figure over a basic valve where x_v is the valve opening, q is the flow of oil, p_1 and p_2 are the pressures.

When deriving the relationship between the flow and pressure the equation for hydraulic forces or, *Bernoulli forces*, can be used in order to describe the force from the fluid. This fluid then flows into the chambers and through the valve orifices. This is described more detailed in [17], but for easier interpretation a more simplified relationship can be derived.

From Figure 3.3 a small perturbation analysis can be done in order to find the relation between flow, pressure, and valve opening. These relations are given by some functions which are shown in Figure 3.4 for illustrative purposes.

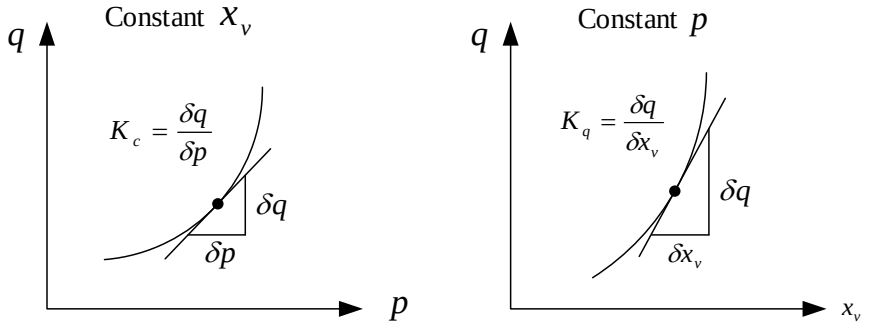

Figure 3.4: Illustrative relation between flow q, pressure p, and valve opening x_v. K_c is the flow-pressure coefficient, and K_q is the flow gain.

Since the flow through the valve is nonlinear it needs to be linearized. Given the above analysis, Equation (3.7) can be linearized at some operating point. Assuming small changes, the following relationship can be derived [26]

$$q_1 = K_q x_v - K_c p_1 \tag{3.8}$$
$$q_2 = K_q x_v + K_c p_2 \tag{3.9}$$

where K_q is the flow gain and K_c is the flow-pressure coefficient. The flow gain and flow pressure are commonly chosen to be a constant when used in modeling of valves.

The valve dynamics can be represented as a second order differential equation given that the nonlinearities in the valve are neglected [9]. The following relationship between the input $u(t)$ (valve input) and output $x_v(t)$ (spool position) holds:

$$\ddot{x}_v(t) + 2\omega_v \delta_v \dot{x}_v(t) + \omega_v^2 x_v(t) = \omega_v^2 u(t) \tag{3.10}$$

Since the available measurements from the valve are pressure at port A and port B, the effective load pressure can then be described as

$$p_{Le}(t) = p_1(t) - \frac{A_1}{A_2} p_2(t) \tag{3.11}$$

3.2 Transfer function model

The equations previously presented could be represented on state space form, but it is more convenient to represent them in transfer function for these types of problems. Transfer functions can give a more detailed explanation for how the system behaves when analyzing them bode plots.

3.2.1 Valve input to valve position

Applying Laplace transform $\mathcal{L}$ on equation (3.10) gives

$$X_v(s) = G_v(s)U(s) \tag{3.12}$$

$$G_v(s) = \frac{\omega_v^2}{s^2 + 2\delta_v\omega_v + \omega_v^2} \tag{3.13}$$

where ω_v is the resonance frequency of the valve, and δ_v the damping.

3.2.2 Valve position and piston position to effective pressure

Applying the Laplace transform on Equations (3.4) and (3.8) give the following expression for the pressure in chamber one, respectively for Equation (3.5) and (3.9) for the pressure in chamber two.

$$P_1(s) = \frac{-A_1 s}{(sC_1 + K_c)}X_p(s) + \frac{K_q}{(sC_1 + K_c)}X_v(s) \tag{3.14}$$

$$P_2(s) = \frac{A_2 s}{(sC_2 + K_c)}X_p(s) - \frac{K_q}{(sC_2 + K_c)}X_v(s) \tag{3.15}$$

$$\tag{3.16}$$

Using the relation from Equation (3.11) the effective load pressure can be described as

$$P_{Le}(s) = -G_1(s)X_p(s) + G_2(s)X_v(s) \tag{3.17}$$

where

$$G_1(s) = \frac{s(A_1/C_{Le})(s + \omega_{e1})}{(s + \omega_1)(s + \omega_2)} \tag{3.18}$$

$$G_2(s) = \frac{(K_q/A_1)(A_1/C_1 + A_2/C_2)(s + \omega_{e2})}{(s + \omega_1)(s + \omega_2)} \tag{3.19}$$

$$\omega_1 = \frac{K_c}{C_1}, \quad \omega_2 = \frac{K_c}{C_2} \tag{3.20}$$

$$\omega_{e1} = \frac{K_c(A_1^2 + A_2^2)}{A_1^2C_2 + A_2^2C_1}, \quad \omega_{e2} = \frac{K_c(A_1 + A_2)}{A_1C_2 + A_2C_1} \tag{3.21}$$

and C_{Le} denotes the effective capacitance defined as

$$\frac{1}{C_{Le}} = \frac{1}{C_1} + \frac{1}{C_2}\left(\frac{A_2}{A_1}\right)^2 \tag{3.22}$$

3.2.3 Effective pressure and external forces to piston position

Taking the Laplace transform $\mathcal{L}$ on the force balance in Equations (3.1) and (3.2), and solve for $X_c(s)$ gives

$$X_c(s) = \frac{B_p s}{(M_1 s^2 + Bs + K)} X_p(s) - \frac{A_1}{(A_1 s^2 + Bs + K)} P_{Le}(s) \tag{3.23}$$

Using the relation of $x_L = x_p + x_c$ from Figure 3.2 together with the previously derived Equation (3.23) the following holds

$$X_p(s) = \left(\frac{((M_1 + M_2)s^2 + Bs + K)A_1}{(M_1 s^2 + Bs + K)(M_2 s^2 + B_p s) + B_p M_2 s^3} \right) P_{Le}(s) \tag{3.24}$$

$$- \left(\frac{(M_1 s^2 + Bs + K)}{(M_1 s^2 + Bs + K)(M_2 s^2 + B_p s) + B_p M_2 s^3} \right) F(s) \tag{3.25}$$

which can be simplified to

$$X_p(s) = G_{pxp}(s) P_{Le}(s) - G_{fxp}(s) F(s) \tag{3.26}$$

where

$$G_{pxp}(s) = \frac{(C_{Le}/A_1)(\frac{s^2}{\omega_{mt}^2} + 2\frac{\delta_{mt}}{\omega_{mt}} s + 1)}{(\frac{s^2}{\omega_{m1}^2} + 2\frac{\delta_{m1}}{\omega_{m1}} s + 1)(\frac{s^2}{\omega_{h2}^2} + 2\frac{\delta_{h2}}{\omega_{h2}} s) + 2\frac{\delta_{h2}}{\omega_{h2}\omega_{m2}^2} s^3} \tag{3.27}$$

$$G_{fxp}(s) = \frac{(C_{Le}/A_1^2)(\frac{s^2}{\omega_{m1}^2} + 2\frac{\delta_{m1}}{\omega_{m1}} s + 1)}{(\frac{s^2}{\omega_{m1}^2} + 2\frac{\delta_{m1}}{\omega_{m1}} s + 1)(\frac{s^2}{\omega_{h2}^2} + 2\frac{\delta_{h2}}{\omega_{h2}} s) + 2\frac{\delta_{h2}}{\omega_{h2}\omega_{m2}^2} s^3} \tag{3.28}$$

and

$$\omega_{m1} = \sqrt{\frac{K}{M_1}}, \quad \delta_{m1} = \frac{B\omega_{m1}}{2K} \tag{3.29}$$

$$\omega_{m2} = \sqrt{\frac{K}{M_2}}, \quad \delta_{m2} = \frac{B\omega_{m2}}{2K} \tag{3.30}$$

$$\omega_{h2} = \sqrt{\frac{A_1^2}{C_{Le} M_2}}, \quad \delta_{h2} = \frac{C_{Le} B_p \omega_{h2}}{2A_1^2} \tag{3.31}$$

$$\omega_{mt} = \sqrt{\frac{K}{M_1 + M_2}}, \quad \delta_{mt} = \frac{B\omega_{mt}}{2K} \tag{3.32}$$

3.3 Block diagram

Combining the transfer functions from the previous section, the following block diagram can be drawn, from valve input $U(s)$ to valve position $X_p(s)$.

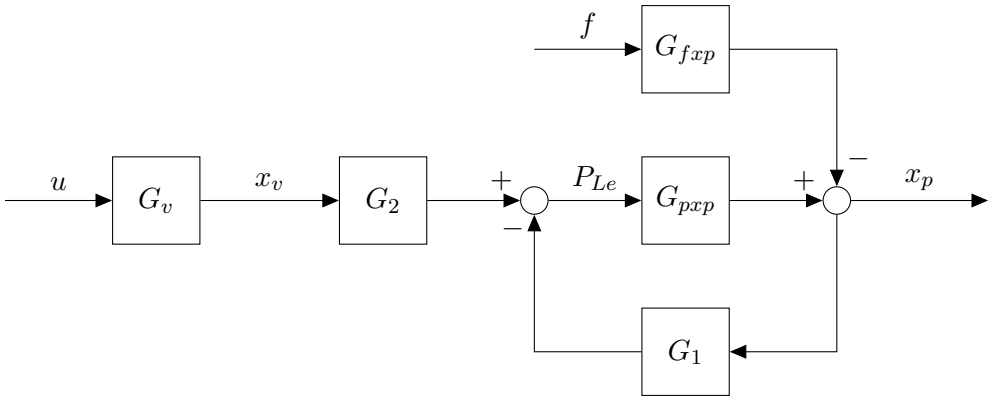

Figure 3.5: Block diagram of the system [20].

From this block diagram the transfer function from valve input $U(s)$ to effective load pressure P_{Le}, with a neglected disturbance f, can be written as

$$P_{Le} = G_{up}(s)U(s) \tag{3.33}$$

$$G_{up}(s) = \frac{G_v G_2}{1 + G_{pxp} G_1} \tag{3.34}$$

It is more interesting to look at the pressure than the actual piston position, since when a hydromechanical system is influenced by a load disturbance, the oscillations will disturb the piston position but the same oscillations will also appear in the pressure. If the oscillations are damped in the pressure, then the rest of the system will be damped as well.

Note that the derived model of the boom function is assumed to be using a double acting cylinder, i.e. in order to lower the crane the pressure in chamber two needs to increase. The boom function can also be used with single acting cylinders, where only the pressure $P_1(s)$ is used to control the function. Single acting cylinders are commonly used on the boom function in order to save energy by only using the gravity to lower the arm. If this is desired to model then Equation (3.17) is replaced with Equation (3.14).

3.4 The swing function

Until now the boom function has been the main focus when deriving the models for the crane. The reason for this is that the boom function can be applied on the other functions, such as the jib and the swing function.

The simplified model of a swing function consists of two hydraulic pistons which are connected to a rotating cylinder. The main difference between a swing function and a boom function is the area relationship for the hydraulic cylinder. A model of a swing function can be seen in Figure 3.6, which then can be translated to an easier interpretation in Figure 3.7

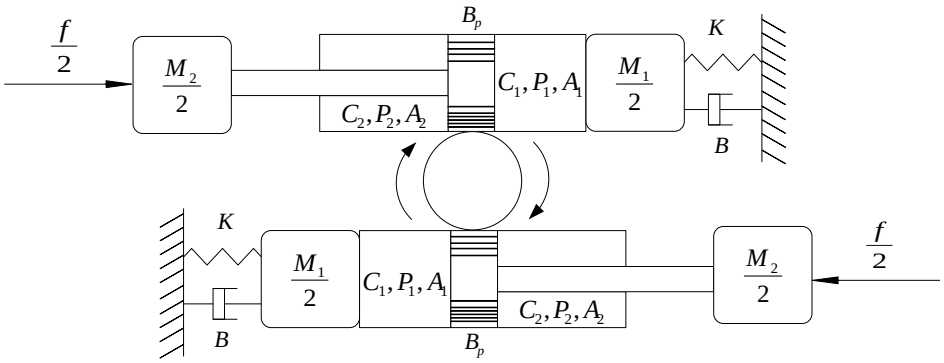

Figure 3.6: Simplified model of a swing function

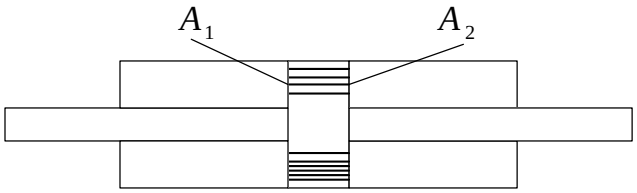

Figure 3.7: The swing function represented as a hydraulic cylinder with two pistons

From Figure 3.7 the area in chamber one and two will be the same, and therefore the swing function will always have the area relationship equal to one. This relationship will only affect the effective load pressure as shown in Equation (3.11). Therefore, the same model that has been derived in this chapter can be used for the swing function by setting $A_1/A_2 = 1$.

This relationship is commonly seen in hydraulic specifications, which are used when designing the valves for which type of function the valve should operate on. This will be the main parameter to set when selecting which function the controller should affect. For instance, when using a single acting boom function the area relationship would be set to 0, since pressure is only applied on one side and therefore, the area on the other side can be neglected.

3.5 Analysis of the model

It is interesting to look at how the derived model behaves for a given input signal and how it changes with different system parameters. This section will provide some analysis of the model in open loop for the boom function and the swing function.

3.5.1 The boom function

One way of doing analysis is to look at the bode plots for the transfer function of the system $G_{up}(s)$. This gives a way to interpret the resonance frequencies of the system. The following Figure 3.8 displays the bode plot of $G_{up}(s)$ where the load disturbance $F(s)$ has been set to zero. The parameters that are used for the model are presented in Appendix A.

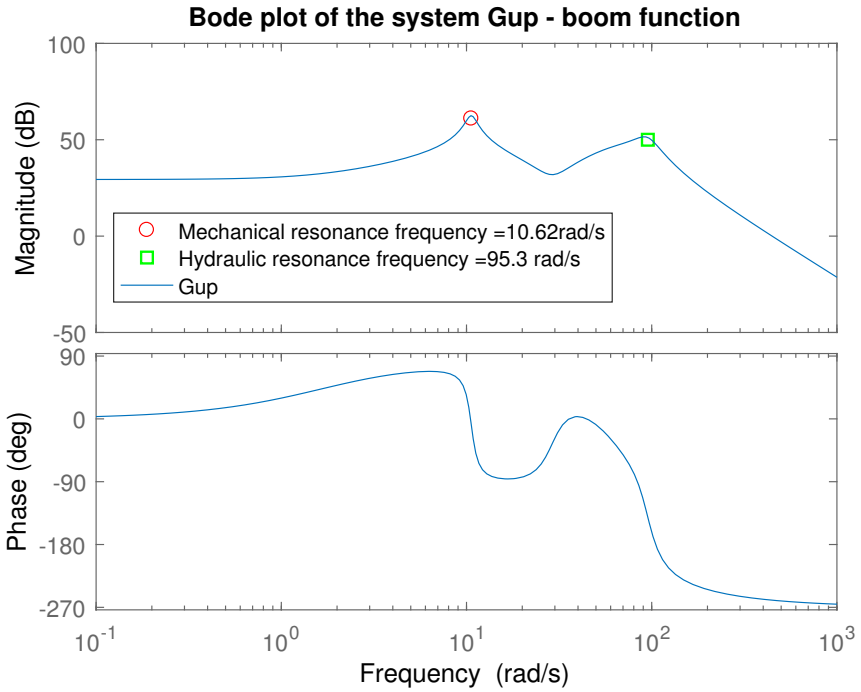

Figure 3.8: Bode plot of the system $G_{up}(s)$ with zero load disturbance.

From the figure above two peaks can be seen, where the first is the resonance frequency from the mechanical system, and the second is from the hydraulic system. If Figure 3.8 is compared with the model in Figure 3.2 the frequency will be caused by the movement of the defined masses.

The mechanical resonance frequency will be the most crucial to dampen, since it is the lowest frequency for the system and will have the most dominating dynamics [17]. When looking at Figure 3.8 the system can be described as a second order transfer function if the hydraulic parts are neglected as

$$G(s) = \frac{\omega_n^2}{s^2 + 2\delta_n\omega_n s + \omega_n^2} \tag{3.35}$$

where ω_n is the resonance frequency and δ_n the corresponding damping ratio for the model.

This is an important property in order to simplify the characteristics of system, seen in Figure 3.9, which will be needed in the control strategy in

Chapter 4. It is also interesting to look at the step response of the system in Figure 3.10, which shows how the effective load pressure oscillates for a given input signal.

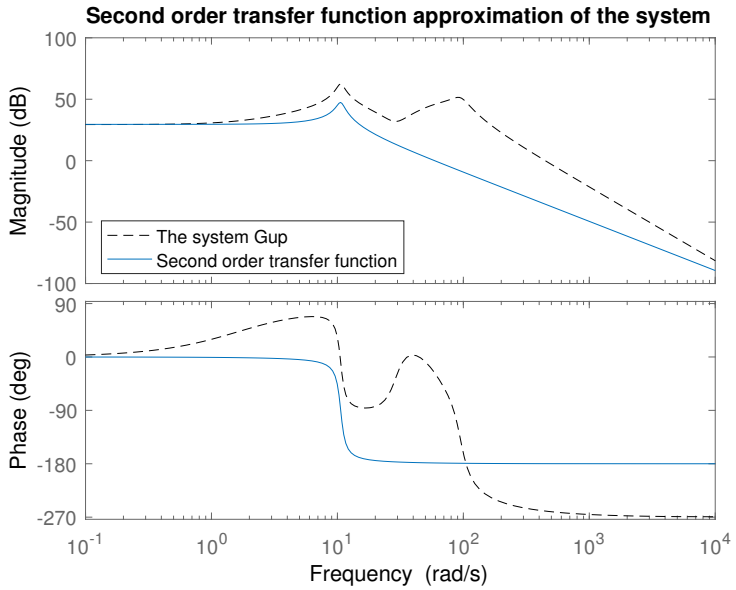

Figure 3.9: Second order transfer function approximation of the system $G_{up}(s)$.

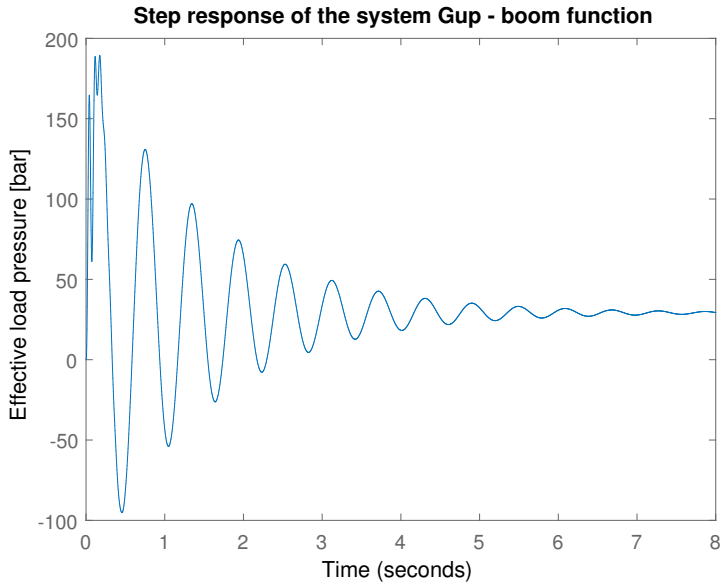

Figure 3.10: Step response of the system $G_{up}(s)$ with zero load disturbance.

3.5.2 The swing function

The swing function will also be analyzed similar to the boom function. The following Figures 3.11 and 3.12 display the bode and the step response of the swing function.

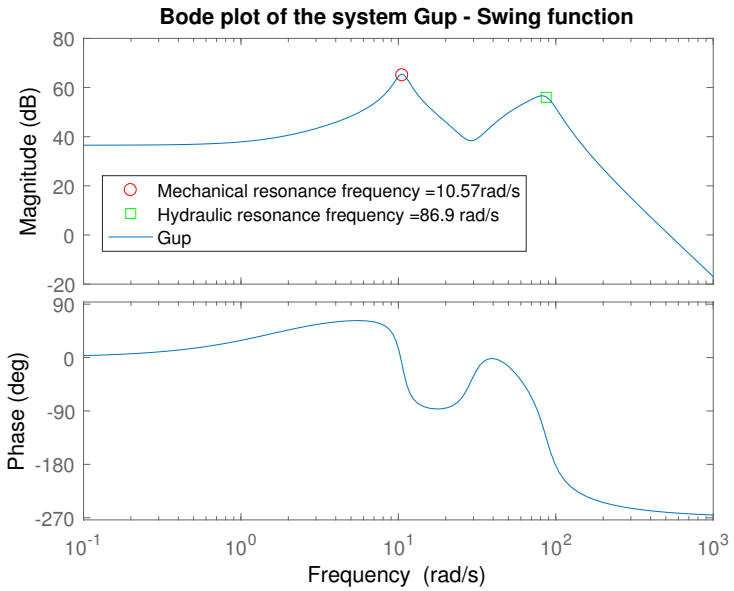

Figure 3.11: Bode plot of the swing function with zero load disturbance.

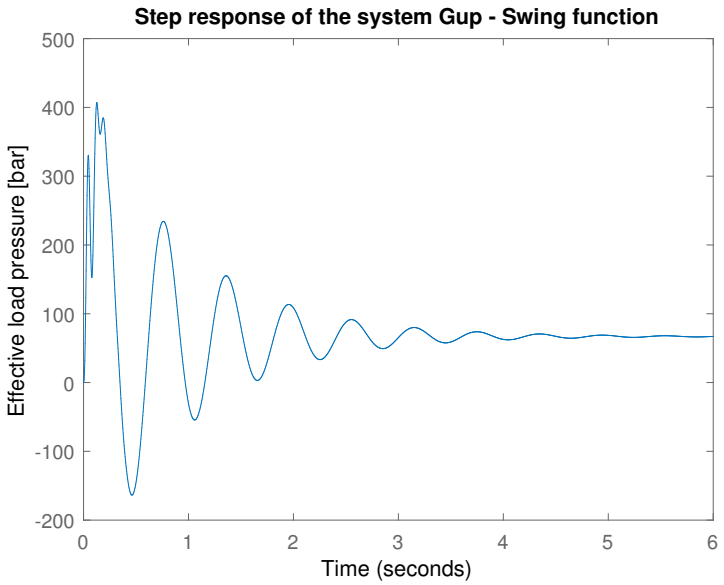

Figure 3.12: Step response of the swing function with zero load disturbance.

The swing function was used with the same parameters as in Appendix A, the difference is that the $A_2 = A_1$ and the areas values are reduced by a factor, in order to lower the pressure amplitude. When comparing the bode plot and the step response with the boom function in Section 3.5.1, there will be a difference in the amplitude and how many oscillations that occur depending on the system parameters. But the general interpretation is that the swing function oscillates less and will be slower, hence lower mechanical resonance frequency compared to the one of the boom function. It should also be noted that the amplitude of the swing functions step response is very high, this is mainly due to the parameters used in the model and can be lowered by increasing the cylinders areas.

3.5.3 Analysis of the resonance frequency

The parameters that are used in the model will affect the mechanical resonance frequency. One parameter that is interesting to vary is the mass M_2, which represents the mass of the cranes arm and the added load disturbance, since different types of machines will have different masses and lengths. This change in mass will be the main reason to the shift of resonance frequencies in the derived model.

In Table 3.1 the increase/decrease of mass M_2, can be seen with its corresponding mechanical resonance frequency. The unloaded case of the crane is set to be at M_2=12 000 kg.

M_2 [kg]	ω_n [rad/s]
10 000	11.49
12 000	10.62
12 200	10.54
14 000	9.91

Table 3.1: The effect of mass M_2 on the resonance frequency.

From Table 3.1, it is clear that the resonance frequency will change for different loads to the crane, which indicates that continuously knowing the frequency will be a crucial part to the active damping solution. If the load on the crane is increased by a small portion, e.g. a wood log around 200 kg, then the change in resonance frequency will not be drastically different to the unloaded cases. It should also be considered that changing the other parameters for the model will also have a major impact on the model. For example, lowering the damping ratio for the valve dynamics will cause the resonance frequency of the valve to have a larger impact on the system, causing more oscillations.

Chapter 4

Control Strategy

After investigating the bode plots in Section 3.5.1 there is now an understanding of which resonance frequency that should be dampened. Therefore, this chapter will be devoted to designing a control strategy in order to dampen the mechanical resonance frequency. The parts of the controller that will be explained is the notch filter, the dynamic pressure feedback, the identifier, and then the complete control solution will be presented with all its parts.

The main difference from the control algorithm that was presented in [20], is that the new controller includes an estimation of the damping of the system, and different filters. A Simulink model have been developed and documented carefully in order to tune the controller in a suitable way, with some influence from [20].

4.1 Discretization

Until now, the derived model has only been shown in continuous form. This is convenient when presenting theories and showing the basic concepts of the system dynamics. However, when implementing a controller in a control unit, the controller needs to be in discrete form. Therefore, this section will treat the discretization for the different parts of the controller.

4.1.1 Discretization method

The method used when discretizing the filters is Tustin's approximation, also called bilinear transformation. This method gives an expression that is replacing the variable s in the continuous transfer functions [4]:

$$s = \frac{2}{T}\frac{(z-1)}{(z+1)} \tag{4.1}$$

where T is the sampling time and z the delay operator.

4.1.2 Pre-warping

When using Tustin's approximation, it is important to pre-warp the frequencies from the discrete function [4]. This transformation will avoid any aliasing and will retrieve the correct frequency after applying Tustin's approximation. This is done by applying the following formula on the modified frequencies.

$$\omega_a = \frac{2}{T} \tan\left(\frac{\omega_d T}{2}\right) \tag{4.2}$$

where T is the sampling time, ω_a continuous analogue frequency and ω_d the modified frequency.

4.2 Notch filter

As discussed in the introduction, oscillations may occur when the operator steers the machine towards the resonance frequency. This can be overcome by filtering the input signals from the operator with the resonance frequency as the break frequency. Such filters are called band-stop- or notch-filter. For a notch filter to work it requires the knowledge of the frequency that should be removed. The notch filter has a second order transfer function:

$$N_f(s) = \frac{s^2 + 2\xi_1 \omega s + \omega^2}{s^2 + 2\xi_2 \omega s + \omega^2} \tag{4.3}$$

where ξ_1 and ξ_2 are parameters that decide how wide and deep the filter will be and ω is the desired frequency to filter, i.e. the mechanical resonance frequency from the machine.

4.3 Dynamic pressure feedback

To avoid that sudden load disturbances, which are common in mobile machines, excites weakly damped modes of the system, a pressure feedback can be used [26]. However, only using a pressure feedback directly will create a static offset for a finite load force and this is not a very good behavior. To cope with this, a dynamic pressure feedback is used. This means that the pressure feedback is filtered so that only oscillations with high frequencies are damped [26]. Dynamic pressure feedback is done by taking the pressure difference P_{Le}(s) from the hydraulic cylinder and filter it with a high-pass or band-pass filter, and multiplying it with a feedback gain K_{fb}. This gain needs to be tuned in order to get a good response of the closed loop system. A feedback gain that is too large will make the closed loop system unstable and a too low gain will make the dynamic pressure feedback ineffective. The filter also needs to be tuned depending on how the system behaves; slow system works well with a high-pass filter while faster system needs a band-pass filter to cope with fast changes in the dynamics. The order of the filter and the break frequencies also need to be tuned for a good damping behaviour. Since

the resonance frequencies are the ones of highest interest it is important to know in what span they exist. Parker Hannifin has been in the industry for a long time and has developed an internal knowledge base of how certain machines behave, and according to their engineering knowledge, the resonance frequencies for the different crane functions lies in the span of 0.5 to 5 Hz.

The dynamic pressure feedback is shown in the form of a block diagram in Figure 4.1.

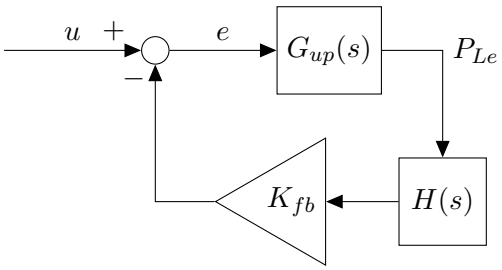

Figure 4.1: The system $G_{up}(s)$ with the dynamic pressure feedback $K_{fb}H(s)$ connected to the controlled input signal.

From the block diagram follows that the closed loop system from input $U(s)$ to output $P_{Le}(s)$ is given by

$$P_{Le}(s) = \frac{G_{up}(s)}{1 + K_{fb}H(s)G_{up}(s)}U(s) \tag{4.4}$$

where K_{fb} is the feedback gain and $H(s)$ is the feedback filter, usually a high-pass filter to dampen out the lower frequencies. A band-pass filter can also be used in order to select a specific band of frequencies to dampen out. Depending on how the system dynamics behaves, different filters might be needed, for instance a second order band-pass filter has shown to have a better damping behaviour in simulations, which will be presented in Chapter 5.

A second order high-pass filter and a second order band-pass filter can be described as the following equations

$$H_{p2}(s) = \frac{s^2}{s^2 + 2\xi\omega_{bh}s + \omega_{bh}^2} \tag{4.5}$$

$$B_{p2}(s) = \frac{s^2\omega_{bl}^2}{(s^2 + 2\xi\omega_{bh}s + \omega_{bh}^2)(s^2 + 2\xi\omega_{bl}s + \omega_{bl}^2)} \tag{4.6}$$

where ξ is the chosen damping ratio between 0 and 1, ω_{bh} is the higher break frequency and ω_{bl} is the lower break frequency.

One thing to note is that dynamic the pressure feedback will always feed back the incoming pressure measurements even if the operator is not steering. This can cause problems if the system is affected by load disturbances when the joystick is left in neutral, which could cause the system to drift. In order to prevent this, a time delay is added to the feedback, as pointed out in [20].

This time delay will delay the operators control signal and include some logic to disable the dynamic pressure feedback when the control signal is inactive. However, this will then tend the controller not to dampen out oscillations that occurs after the operator has left the joystick in neutral position.

4.4 Parameter identification

The main idea of the controller is to find the resonance frequency and the damping of the system and then use it to feed into the notch filter and pressure feedback. In order to accomplish this, an identification will be needed to find the unknown mechanical resonance frequency and the damping of the system.

4.4.1 Recursive least squares method (RLS)

One of the most common identifier is the recursive least squares algorithm. The algorithm calculates a vector of parameters that minimizes the mean square error, given that the input and output of the system can be measured. The basic idea of the RLS method is to minimize the criterion

$$V_N\left(\theta(t)\right) = \frac{1}{N}\sum_{t=0}^{N}\Big(y(t) - \varphi(t)^T\theta(t)\Big)^2 \tag{4.7}$$

which is the mean square error, where $\theta(t)$ is the parameters, $y(t)$ is the measurement, in this case it will be the effective load pressure and $\varphi(t)$ is the regression vector. In order to find the parameter vector and the regression vector, the Equation (4.15) can be written as an ARX-model (Auto-Regressive with eXogenous input), such as

$$y(t) = b_0u(t) + b_1u(t-1) + b_2u(t-2) + a_1y(t-1) - a_2y(t-2) \tag{4.8}$$

which then forms the parameter and regression vectors accordingly

$$y(t) = \varphi(t)^T\theta(t) \tag{4.9}$$

$$\theta(t) = \begin{bmatrix} a_1 & a_2 & b_0 & b_1 & b_2 \end{bmatrix}^T \quad \varphi(t) = \begin{bmatrix} y(t-1) \\ -y(t-2) \\ u(t) \\ u(t-1) \\ u(t-2) \end{bmatrix} \tag{4.10}$$

The Equation 4.7 is then solved recursively; the algorithm is described in [6], and is a modified version of the original algorithm, which is commonly found in basic control literature and supplements as in [27]. The equations for the modified version is summarized in Equation (4.11).

$$
\begin{aligned}
&\textit{The RLS-algorithm} \\
&\hat{\theta}(t) = \hat{\theta}(t-1) + a(t)K(t)\epsilon(t) \\
&\varepsilon(t) = y(t) - \varphi^T(t)\hat{\theta}(t-1) \\
&K(t) = P(t)\varphi(t) \\
&P(t) = \frac{1}{\lambda(t)}\left(P(t-1) - a(t)\frac{P(t-1)\varphi(t)\varphi^T(t)P(t-1)}{\lambda(t) + \varphi^T(t)P(t-1)\varphi(t)}\right)
\end{aligned}
\tag{4.11}
$$

The algorithm consist of the estimated parameters $\hat{\theta}(t)$, the regression vector $\varphi(t)$, the prediction error $\varepsilon(t)$, the correction gain vector $K(t)$, the forgetting factor $\lambda(t)$, and the covariance matrix $P(t)$. In the original RLS-algorithm the forgetting factor is a value in the interval $0 \leq \lambda(t) \leq 1$, which gives exponentially less weight to older measurements. Smaller value gives a good ability to follow the varying dynamics, but it will increase the sensitivity to disturbance.

The dynamics in mobile machines can vary with its operating point and therefore, the RLS method needs to be able to handle changes. The traditional way of selecting a constant forgetting factory is not sufficient and it needs to be modified in the following way

$$\lambda(t) = 1 - (1 - \lambda_0)\left(1 - \frac{\Gamma(t)}{\gamma_{max}}\right) \tag{4.12}$$

where λ_0 usually is between 0.9 and 0.99, $\Gamma(t)$ is the trace of $P(t)$ and γ_{max} is the upper bound of the trace. When describing the forgetting factor in this way it will ensure that the covariance $P(t)$ stays bounded and when the trace reaches its upper limit, the forgetting factor will tend to one, meaning that the RLS-algorithm will weight all values equally [6].

The variable $a(t)$ in the RLS equation is a variable for turning off the update of the parameters. This needs to be implemented since when the operator stops steering the machine or when the system is inactive, the covariance of the algorithm may explode when time increases. In order to avoid this, the variable $a(t)$ should be calculated as suggested in [6]

$$a(t) = 1 - \frac{\Gamma(t)}{\gamma_{max}}\lambda_0 \tag{4.13}$$

This means that when $\Gamma(t)$ is large, i.e. the covariance is high, $a(t)$ will decrease, making the estimation less affected by the inactive system. Note that using this way of calculating $a(t)$ the variable will never be equal to zero and this is desirable since otherwise it would turn off the recursive algorithm completely.

An alternative would be to set the variable $a(t)$ to be on or off depending on the control signal, for instance

$$\begin{cases} a(t) = 1, & |u(t)| > d \\ a(t) = 0, & \text{otherwise} \end{cases} \tag{4.14}$$

where d is a lower bound value for the operator control signal. In mobile machines, there is always a dead-band which is applied on the operator control signal for safety reason. This is usually set to be around 5-10 %. Therefore, everything below this value will be treated as zero, and the RLS-algorithm can be turned on and off. The latter method of calculating $a(t)$ has been used in this project for easier implementation.

In order to retrieve the frequency and the damping ratio, a model of how the system behaves is needed. As mentioned in Section 3.5.1 the hydromechanical system can be approximately described as a second order transfer function in Equation (3.35).

Since the RLS-algorithm only works on discrete form, the above equation needs to be discretized, and this is done using Tustin's approximation as previously discussed in Section 4.1. Applying the Equation (4.1) in Equation (3.35) yields

$$G(z) = \frac{T^2\omega_n^2 + 2T^2\omega_n^2 z^{-1} + T^2\omega_n z^{-2}}{(T^2\omega_n^2 + 4\delta_n T\omega_n + 4) + (2T^2\omega_n - 8)z^{-1} + (T^2\omega_n^2 - 4\delta_n T\omega_n + 4)z^{-2}} = \\ = \frac{b_0 + b_1 z^{-1} + b_2 z^{-2}}{1 - a_1 z^{-1} + a_2 z^{-2}} \tag{4.15}$$

where b_0, b_1, b_2, a_1, and a_2 are the parameters that will be estimated by the RLS. From these parameters the expression for ω_n and δ_n can be derived

$$\omega_n = \sqrt{\frac{4(a_2 - a_1 + 1)}{T^2(a_1 + a_2 + 1)}} \tag{4.16}$$

$$\delta_n = \frac{T^2\omega_n^2(1 - a_2) + 4(1 - a_2)}{4T\omega_n(a_2 + 1)} \tag{4.17}$$

where ω_n is the mechanical resonance frequency and δ_n the damping of the system. Where the damping of the system will be used to determine the width of the notch filter, i.e ξ_1.

4.4.2 Kalman filter parameter estimation

The RLS-algorithm is not the only method when it comes to identification and therefore a comparison with the Kalman filter estimation has been done. The main difference between Kalman and the RLS is that the Kalman filter will include the assumption of that the parameters are affected by process noise and measurement noise. The benefits from the Kalman filter is that measurement noise and different changes in the system can be taken care of. Compared with the RLS-algorithm which converges faster and has less noise [21].

The system that is given in Equation (3.35) can be described by a discrete state-space representation as

$$x(k+1) = A(\theta)x(k) + B(\theta)u(k) + w(k) \tag{4.18}$$
$$y(k) = C(\theta)x(k) + v(k) \tag{4.19}$$

where θ are the parameters that will be estimated, $w(k)$ is the process noise, and $v(k)$ is the measurement noise.

The Kalman filter can then be formulated as.

The Kalman filter

$$\begin{aligned}
\hat{x}(k+1) &= \hat{x}(k) + K(k+1)\varepsilon(k+1) \\
\varepsilon(k+1) &= y(k) - \varphi(k+1)^T\hat{x}(k) \\
K(k+1) &= P(k+1)\varphi^T(k+1) \\
P(k+1) &= P(k) - \frac{P(k)(k+1)\varphi^T(k+1)P(k)}{R + \varphi^T(k+1)P(k)\varphi(k+1)} + Q
\end{aligned} \tag{4.20}$$

where R is the measurement noise, $\varepsilon(k)$ is the prediction error and Q is the covariance of the process noise. The states vector $\hat{x}(k+1)$, and the measurement vector $y(k)$ can be seen as

$$\hat{x}(k+1) = x(k) + w(k), \quad \mathbb{E}(w(k)) = Q \tag{4.21}$$
$$y(k) = \varphi(k)^T x(k) + v(k), \quad \mathbb{E}(v(k)) = R \tag{4.22}$$
$$x(k) = \begin{bmatrix} a_1 & a_2 & b_0 & b_1 & b_2 \end{bmatrix} \tag{4.23}$$

where $x(k)$ will be the vector containing the paramters.

4.4.3 Pre-filters

The identification method will be sensitive to disturbances and therefore some pre-filters need to be used for the input as well as the output signal. It is suggested in [8] to use filter in a specific frequency band. This frequency band should be in the range of the resonance frequency interval $0.5 - 5$Hz.

One solution to this is to implement a band-pass filter on the signals into the identifier. It is also important to select a filter that has higher order than the system dynamics, so that all of the state derivatives are low pass filtered. Since the system can be described as a second order transfer function, the suggested filter will therefore be of third order. The idea of using a band-pass filter is that the benefits from the low- and high-pass characteristics can be utilized. The low-pass part will take care of unwanted measurement noise from the output and the high-pass part will enable us to look more closely to the resonance frequency.

The third order band-pass filter can be described as third order low-pass filter multiplied with a third order high-pass filter in the s-domain. The equation for the band-pass filter is given below in continuous time.

$$B_{p3}(s) = \frac{s^3\omega_{bl}^3}{(s^3 + 2s^2\omega_{bh} + 2s\omega_{bh}^2 + \omega_{bh}^3)(s^3 + 2s^2\omega_{bl} + 2s\omega_{bl}^2 + \omega_{bl}^3)} \tag{4.24}$$

where ω_{bl} is the lower break frequency and ω_{bh} is the high break frequency. According to [20] a rule of thumb is that the higher break frequency should be 0.5 times the resonance frequency of the system, and the lower frequency should be a factor times the resonance frequency. This is based on [8] where the mechanical frequency is usually in the range of one or two decades, which means that the lower and upper break frequency should be selected as

$$\omega_{bl} = 30\omega_{bh} \tag{4.25}$$

and that ω_{bl} must be less than the Nyquist frequency , $1/(2T)$. This however are just suggestions and the upper and lower break frequencies can first be set to the condition in Equation (4.25), and then tested in simulation to see if the values needs to be adjusted.

4.5 Complete controller

The complete controller consists of the notch-filter, the pre-filters, RLS identifier, and the dynamic pressure feedback. The following figure 4.2 displays how the complete control strategy looks in a block diagram.

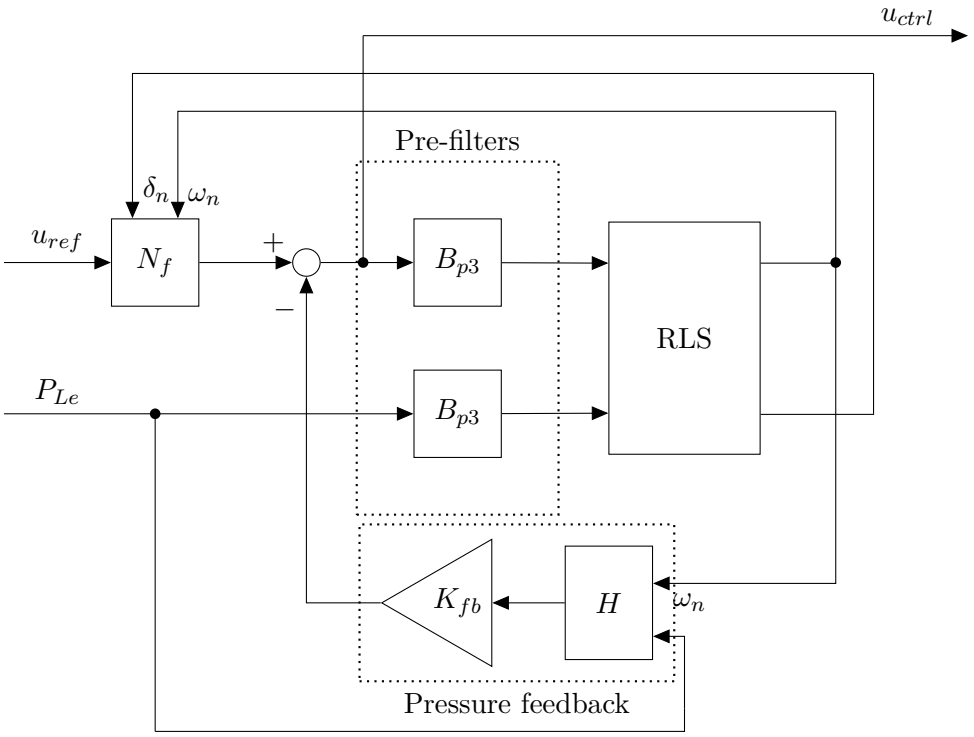

Figure 4.2: Figure over the complete control scheme.

Here N_f is the notch-filter, B_{p3} is the third order band-pass filter, H the dynamic pressure feedback filter, P_{Le} is the effective load pressure, u_{ref} is the signal from the operator, often referred to as the command signal and u_{ctrl} is the adapted control signal. This control strategy will be adaptive and needs less tuning than the controller in [20]. The main tuning of the controller will be the feedback gain K_{fb} and the type of feedback filter H and its filter settings. Tuning might be necessary depending on which function the controller will operate on and on what type of machine.

Chapter 5

Simulation of the Controller

This chapter will present the simulations with the derived mathematical models together with the adaptive controller. The simulations will be done by implementing the mathematical model and the control structure in Simulink. The parameters used for the models in the simulations are presented in Appendix A.

5.1 The boom function

The simulation of the boom function will first be done by assuming that the resonance frequency and the damping are known, and then the boom function will be simulated when using the RLS-algorithm.

5.1.1 Simulation with known resonance frequency

When the resonance frequency and the damping are known, the notch-filter will perform perfectly, and the tuning lies in selecting a good filter, and feedback gain for the dynamic pressure feedback. The boom function has been simulated in open loop and then plotted in a bode plot together with the effect of only using the notch-filter, and then with only using the pressure feedback. The result can be seen in figure 5.1. The step response for the system when only using a notch filter and the dynamic pressure feedback separately is displayed in Figure 5.2, where the damping effect can be seen directly in the effective load pressure.

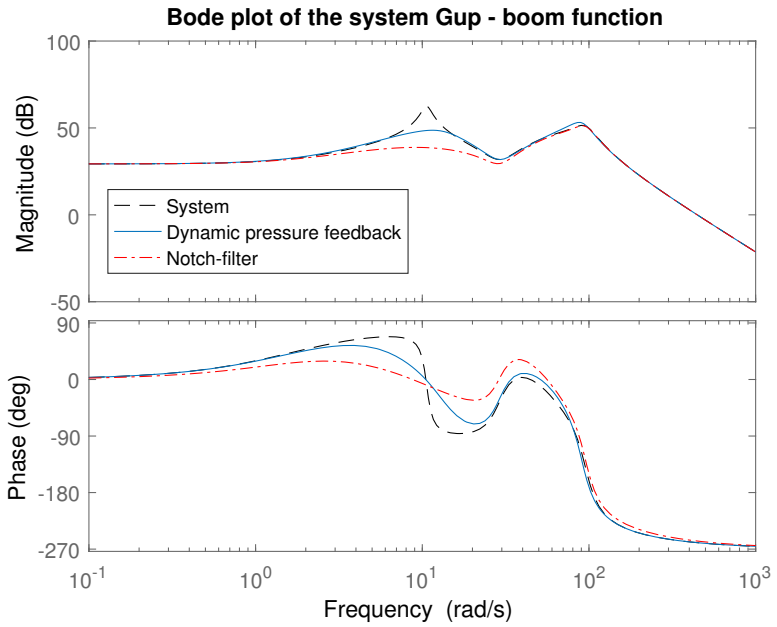

Figure 5.1: Bode plot of the boom function, comparing the effect of the different filter parts of the control setup.

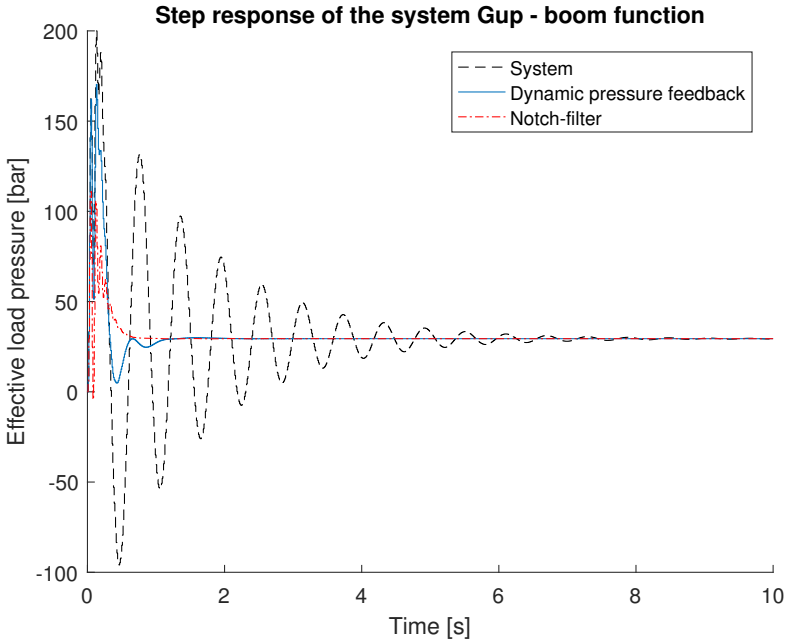

Figure 5.2: Step response of the boom function, comparing the effect of the different filter parts of the control setup.

For the dynamic pressure feedback a second order band-pass filter was used with the damping ratio set to $\xi = \sqrt{2}/2$ and the feedback gain was set to $K_{fb} = 3.5 \cdot 10^{-3}$. The notch filter has a better damping effect than the pressure feedback. However, the pressure feedback can dampen load disturbances that act on the crane, which the notch filter cannot do. When combining the notch filter and the pressure feedback, in Figure 5.3, the result is very high damping on the mechanical resonance frequency. The tuning of the control algorithm is very difficult and always results in an over-damped system when looking at the closed loop bode plots. In order to make it less over-damped the feedback gain could be decreased but then the effect of the pressure feedback would decrease as well. Therefore, there is a trade-off between an over-damped system and the effect of the pressure feedback. As mentioned in [20] the control system needs to be tuned in order to avoid this over damped behaviour. This can be done by changing, for example, the depth of the notch-filter. However, it will make the impact of the notch filter less significant, and hence there is a trade-off between how much the notch filter and the pressure feedback will affect the system.

When the system gets over-damped, the phase of the system will be twisted, and creating a phase shift that is different to the original phase of 90° at the mechanical resonance frequency. This will make a shift in the pressure when the controller is used. In the simulations it is not that obvious, but it can be seen much clearer in the experiments in Chapter 7. This phase shift should be considered when tuning the controller, since it will affect the response of the system, making it feel slower if the phase shift is too large.

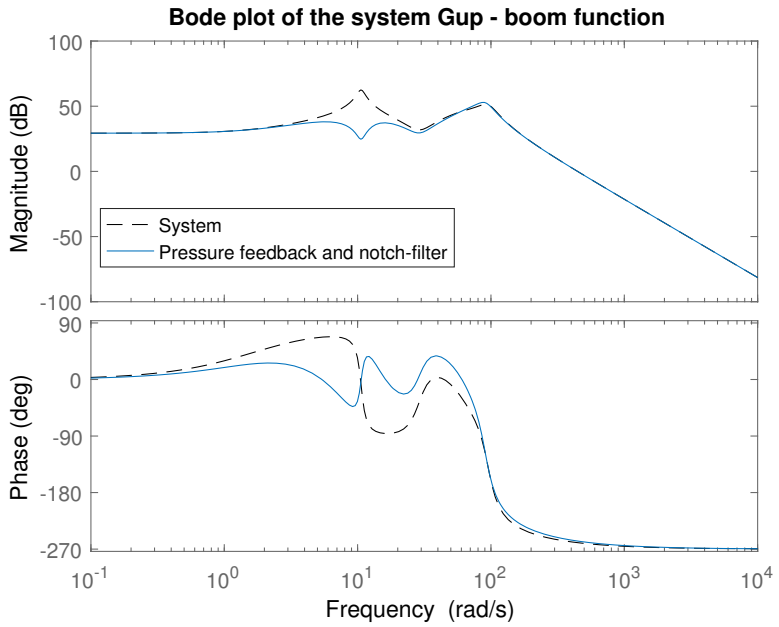

Figure 5.3: Bode plot of the boom function, comparing the effect of the complete control setup.

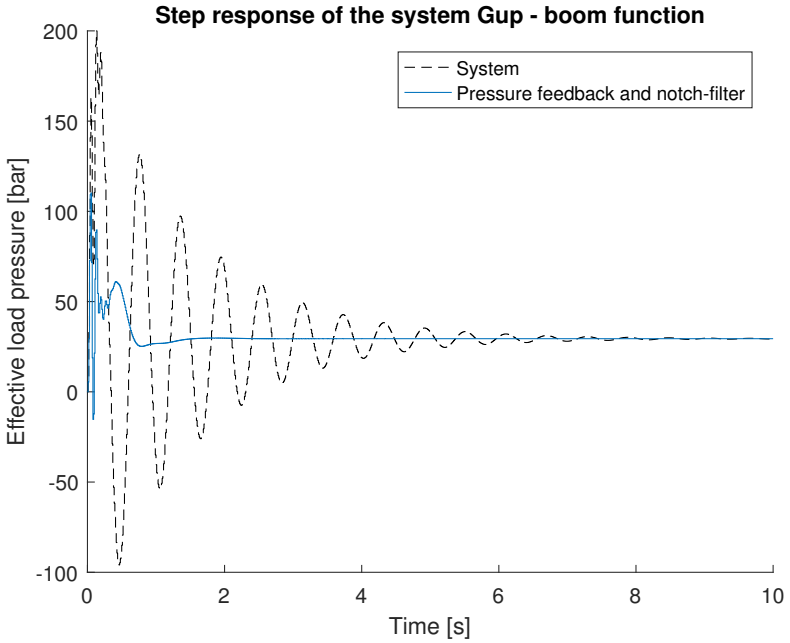

Figure 5.4: Step response of the boom function, comparing the effect of the complete control setup with known system parameters.

When looking at a step response for the complete system, the damping effect of the effective load pressure can be seen much clearer in Figure 5.4. Note that in the beginning the pressure is a bit spiky, and this is due to the resonance from the hydraulic system since that frequency is not dampened. One thing that needs to be consider when looking at the Figures in 5.3 and 5.4 is that the applied control signal is not saturated, i.e. the control signal is allowed to be higher or lower than what is possible to steer in a real application. This is solved by limiting the control signal with a saturation from -1 to 1, i.e. -100% to 100%. Figure 5.5 shows the damping effect when the saturation is used and the applied control signal.

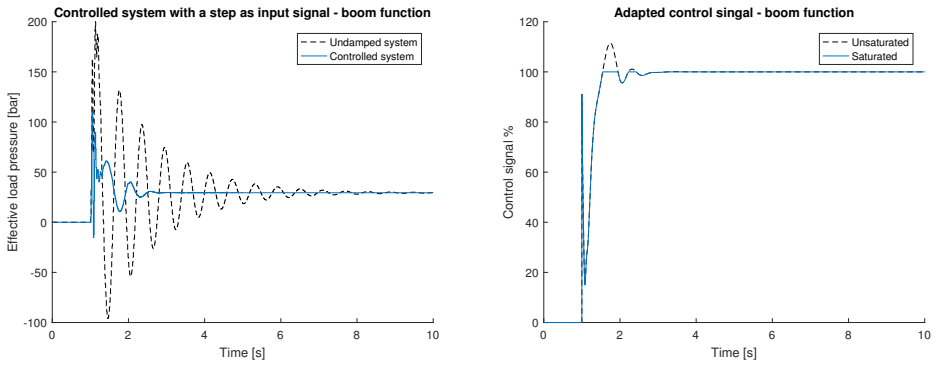

Figure 5.5: Step response of the controlled system with the saturated control signal.

For these simulations the dynamic pressure feedback has been used with a second order band-pass filter, in [20], a first order high-pass filter was used. The effect from the high-pass filter will result in a poor damping behaviour from the dynamic pressure feedback, making it perform badly when additional load disturbances are added to the system. The effect of using a first order high-pass filter on the system is shown in Appendix B.

5.1.2 Simulation with the RLS identifier

When using the RLS identifier the same settings for the band-pass filter in the pressure feedback and the feedback gain was used as in Section 5.1.1. The main difference is now to tune the RLS identifier so that the estimated resonance frequency and the damping ratio gets close to the desired values, and that they converge quickly. Figure 5.6 displays the result for the controlled system compared to the undamped system, where the system and the RLS-identifier uses a sampling time of 0.01s.

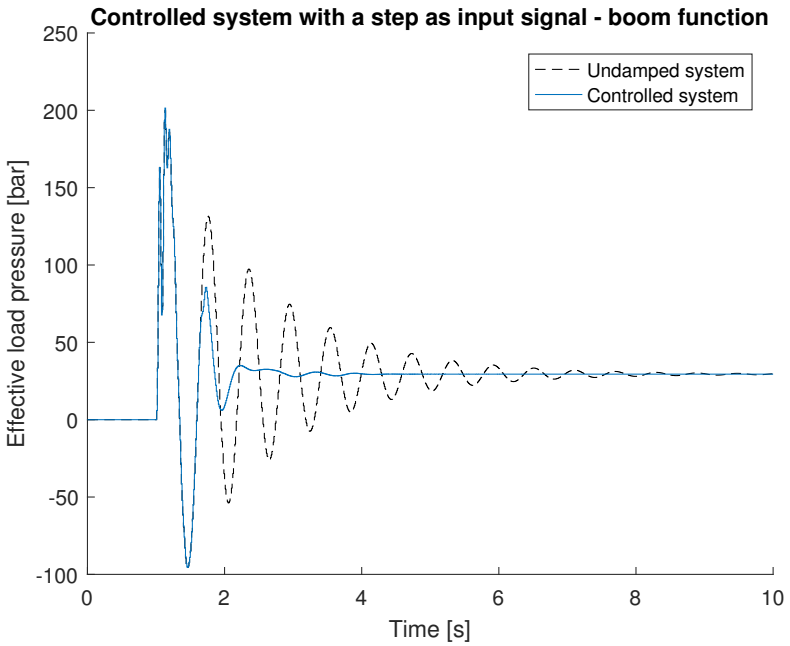

Figure 5.6: Step response of the boom function comparing the effect of the complete control setup when the RLS identifier is used.

Comparing Figure 5.6 with figure 5.4 they will differ since the estimated frequency and the damping needs to converge to their desired values. Therefore, the effect of the controller is not seen immediately. The estimated frequency can be seen in Figure 5.7 where a saturation has been used from $0.5 \cdot 2\pi$ rad/s to $3 \cdot 2\pi$ rad/s, which corresponds to the resonance frequency interval in order to prevent high estimates in the beginning. The estimated damping ratio is presented in Figure 5.8 where a saturation has been set to be between 0 and 1.

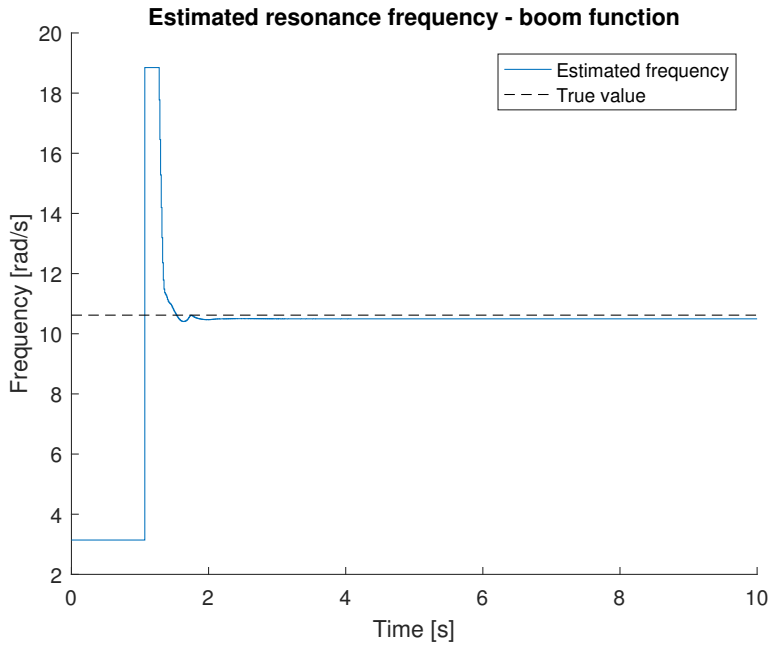

Figure 5.7: The estimated frequency where $\gamma_{max} = 1000$ and $\lambda_0 = 0.99$ for the RLS identifier. The estimated frequency converges to $\omega_n = 10.5$ rad/s.

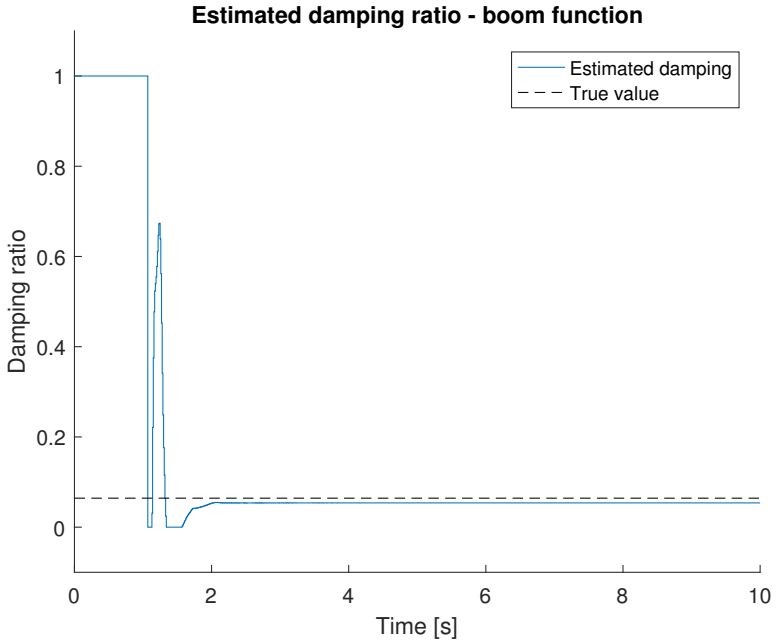

Figure 5.8: The estimated damping where $\gamma_{max} = 1000$ and $\lambda_0 = 0.99$ for the RLS identifier. The estimated damping converges to $\delta_n = 0.0537$.

The identifier for the boom function performs quickly with a settling time around 2 seconds and has a decent accuracy. The estimated frequency converges to $\omega_n = 10.5$ rad/s where the true value is $\omega_n = 10.62$rad/s, and the estimated damping converges to $\delta_n = 0.0537$ and the true value is $\delta_n = 0.0643$. Since the identifier is based on a simplified model of the system, there will be some error with accuracy on the estimates.

The basic tuning method for the RLS identifier is to set the λ_0 value in the range of 0.9-0.99, where it is commonly set to 0.99. Depending on how fast the estimate of the parameters should be, the upper limit of the covariance γ_{max} can be changed to speed up or slow down the estimates convergence. This can be seen in Figure 5.9 where the result of changing the value from 1 to 1000 is displayed.

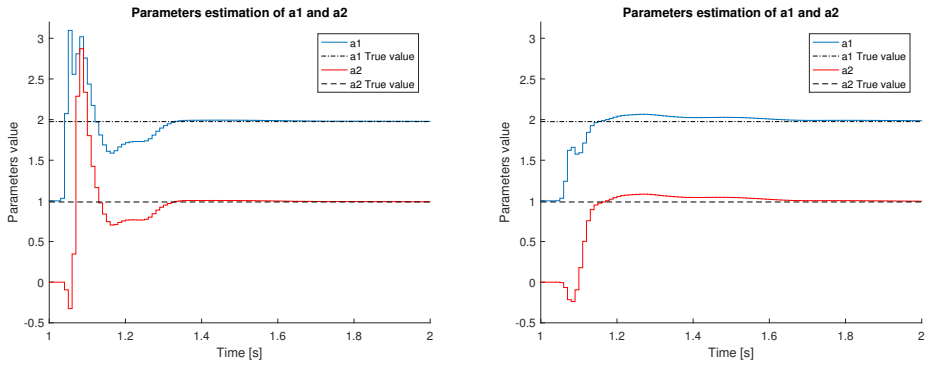

Figure 5.9: Figures over the estimated parameters for $\gamma_{max} = 1000$ (left) and $\gamma_{max} = 1$ (right)

Even though the estimation with $\gamma_{max} = 1$ seems to converges to its parameter true value there is still a small error which will then reflect upon the calculated frequency, making the complete algorithm perform worse.

5.1.3 Simulation with the Kalman filter identifier

The system has been tested with a Kalman filter for the estimation of the resonance frequency and the damping ratio, and the step response is displayed in Figure 5.10. The estimated frequency can be seen in Figure 5.11, and the damping ratio in Figure 5.12 where the selected filter and feedback gain was set to the same values as for the RLS identifier as in Section 5.1.2. For the Kalman identifier, the tuning differs from the RLS-algorithm, it uses constant covariance matrices where the RLS uses initial tuning values that then changes over time. This means that the RLS will handle varying system dynamics better than the Kalman filter does in mobile machines. The Kalman filter has also problem with change of input signal, e.q. a ramp function instead of a step, making the filter perform worse with the same tuning parameters.

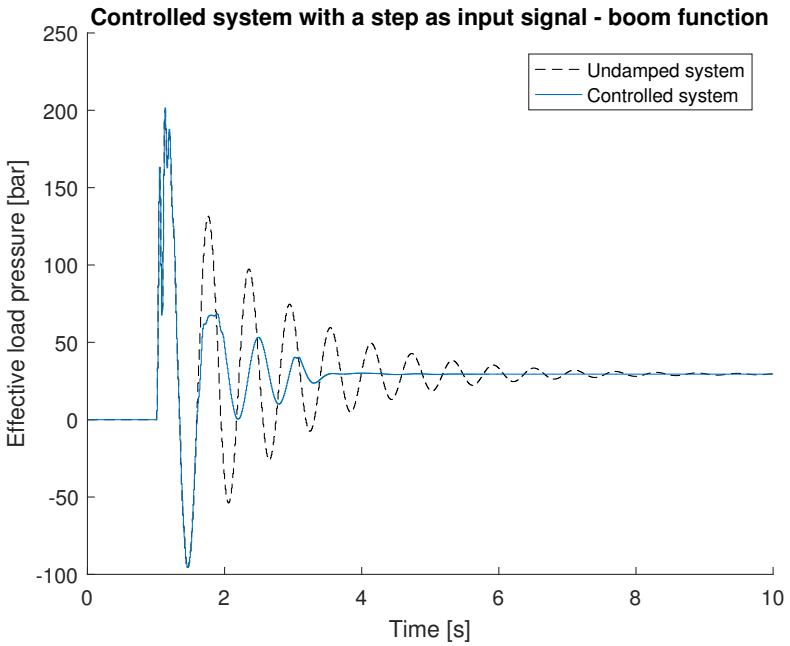

Figure 5.10: Step response of the boom function showing the effect of using a Kalman filter for the identification.

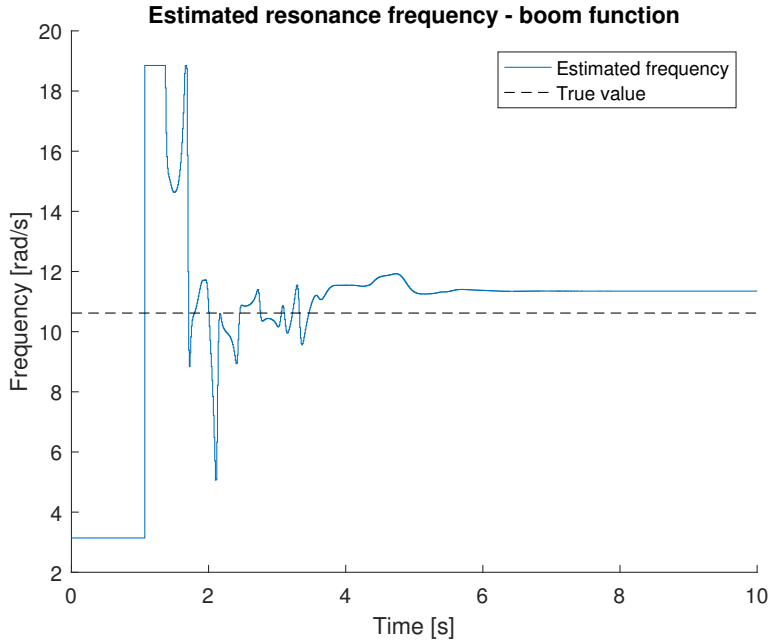

Figure 5.11: The estimated frequency where the values $R = 0.99$, $Q = 1 \cdot 10^{-3}$ and $P = 1000$ has been used for the Kalman identifier. The estimated frequency converges to $\omega_n = 11.35$ rad/s

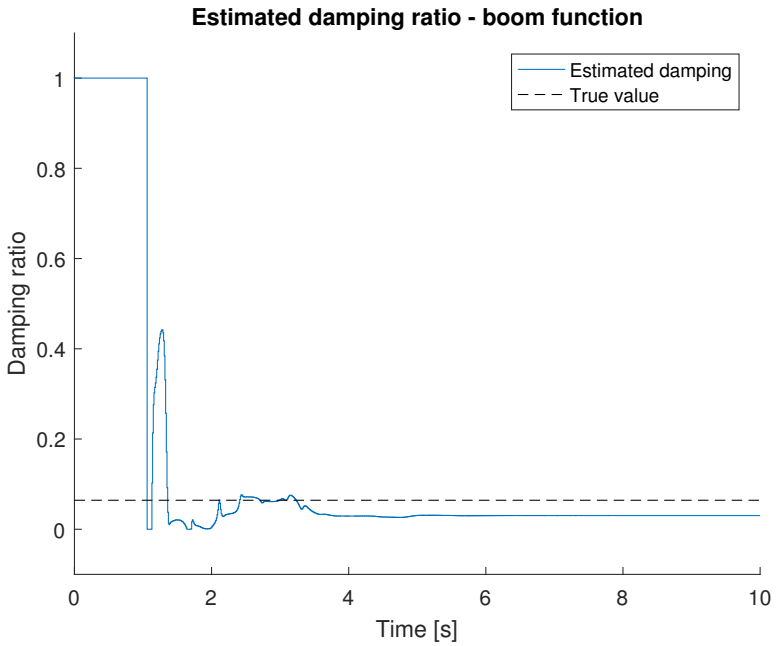

Figure 5.12: The estimated damping where the values $R = 0.99$, $Q = 1 \cdot 10^{-3}$ and $P = 1000$ has been used for the Kalman identifier. The estimated damping converges to $\delta_n = 0.030$.

The estimated frequency converges to $\omega_n = 11.35$ and the damping $\delta_n = 0.030$ where the true values are $\omega_n = 10.62$ rad/s and respectively $\delta_n = 0.0643$. The estimation of the frequency and the damping ratio are much worse than the ones from the RLS identifier, yet the active damping still performs rather well as seen in Figure 5.10. This is a strong indication of how good the pressure feedback can be to the system even if the estimated frequency and damping are not accurate.

5.2 The swing function

The simulation of the swing function will first be done by assuming that the resonance frequency and the damping are known and then it will be compared when an identifier is used to estimate the frequency and the damping ratio. The same tuning parameters that was used for the boom function have been used here as well, the only difference is the feedback gain is set to $k_{fb} = 1.5 \cdot 10^{-3}$.

5.2.1 Simulation with known resonance frequency

The bode plot of the different parts of the controller for the swing function shown in Figure 5.13, and the effect of the complete controller in Figure 5.14.

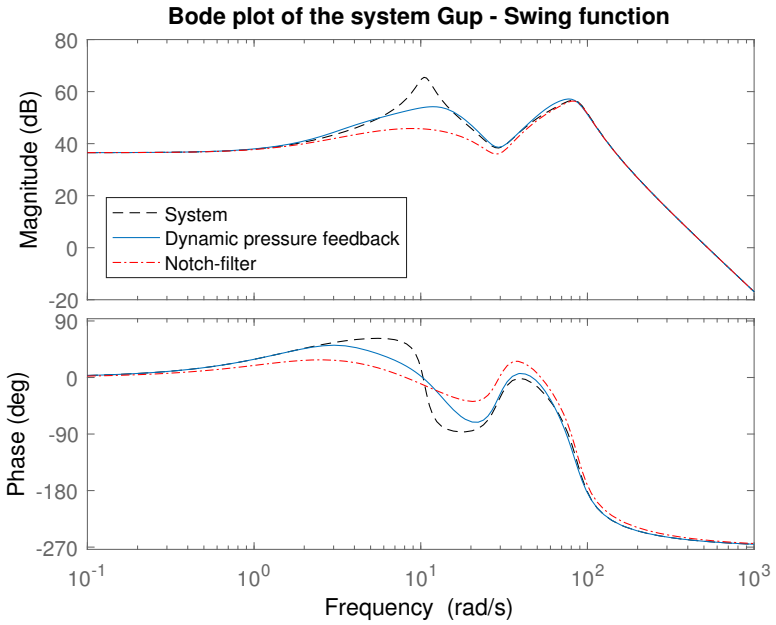

Figure 5.13: Bode plot of the swing function comparing the effect of the different filter parts of the control setup.

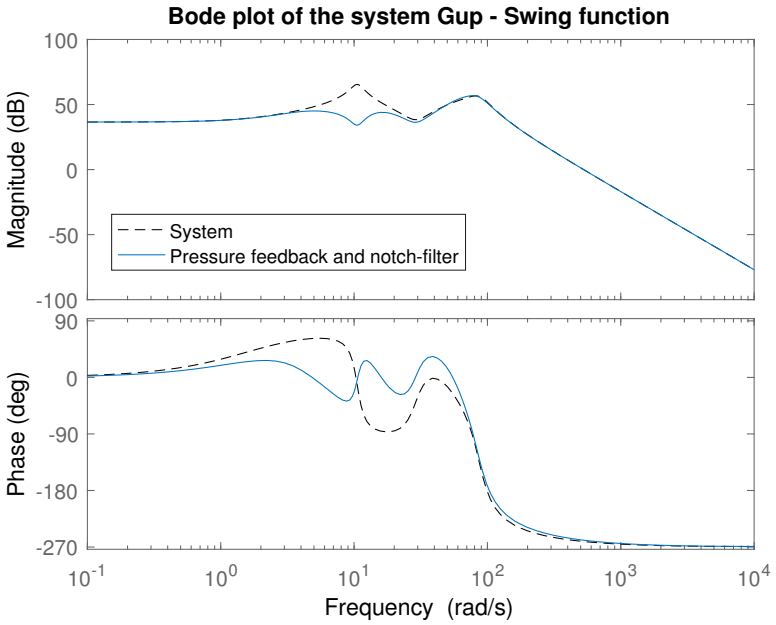

Figure 5.14: Bode plot of the swing function comparing the effect of the complete control setup.

The main difference between the bode plots of the boom function and the swing function is that the systems amplitude will be higher for the swing function, and it will oscillate less. The overall effect of the controller will have similar result when using the derived model of the crane.

To get a better understanding of the actual damping effect on the swing function the step response for each part of the controller is shown in Figure 5.15, and the step response for the complete controller in Figure 5.16.

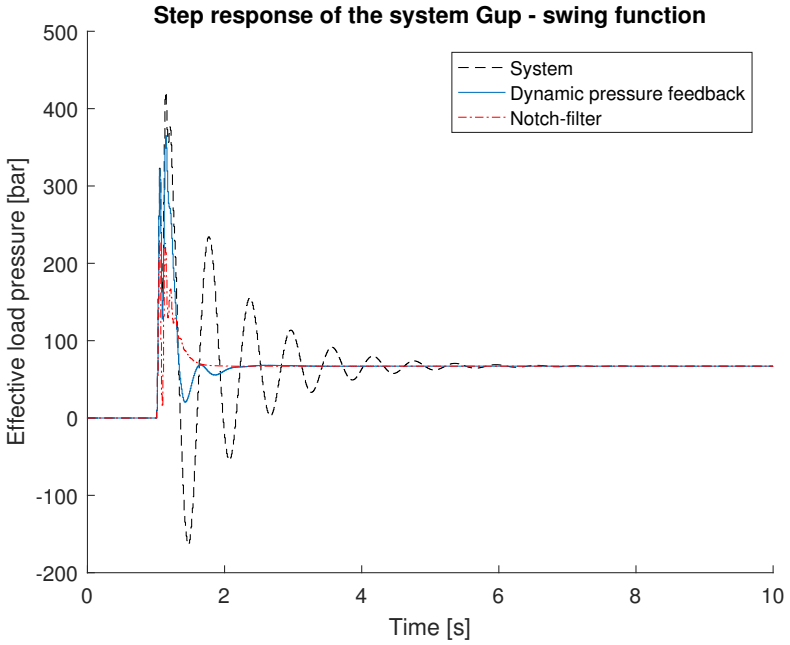

Figure 5.15: Step response of the swing function comparing the effect of the different filter parts of the control setup.

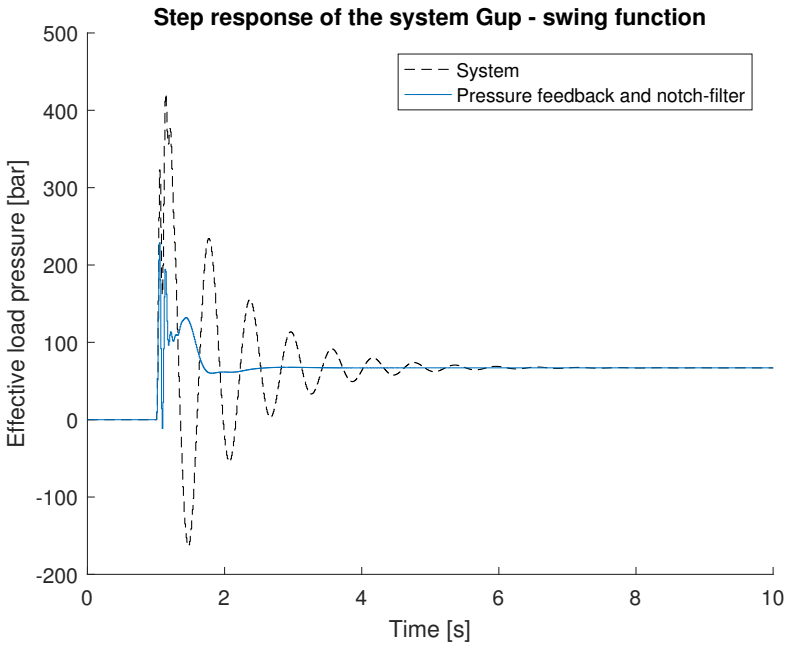

Figure 5.16: Step response of the swing function comparing the effect of the complete control setup.

As previously done in Section 5.1.1, it is interesting to see how the effect of the controller will be when the control signal is limited to -100% to 100%. The behaviour of the system and the saturated control signal can be seen in Figure 5.17.

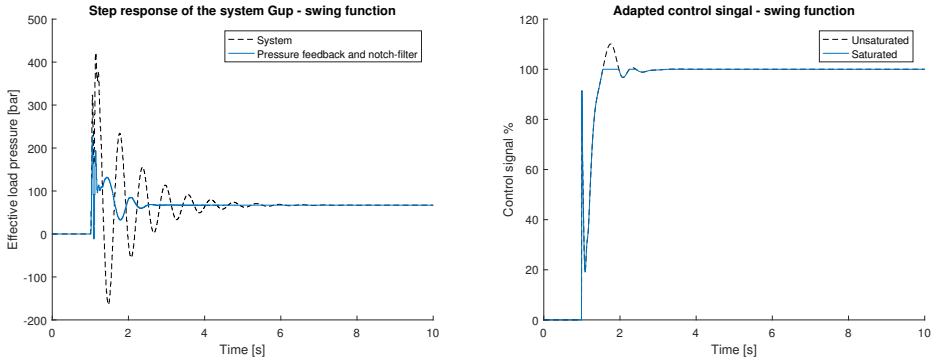

Figure 5.17: Figures over the controlled system with the saturated control signal

When the resonance frequency and the damping ratio are known for the system, the damping effect will be good for the swing function. The swing function will oscillate less, due to the lower mechanical frequency.

5.2.2 Simulation with the RLS identifier

For the case when the resonance frequency and the damping ratio is not known the effect of the controller will be different. The same settings from the RLS identifier are set to be the same as in the boom function cases, i.e. $\gamma_{max} = 1000$ and $\lambda_0 = 0.99$, the damping effect can be seen in Figure 5.18.

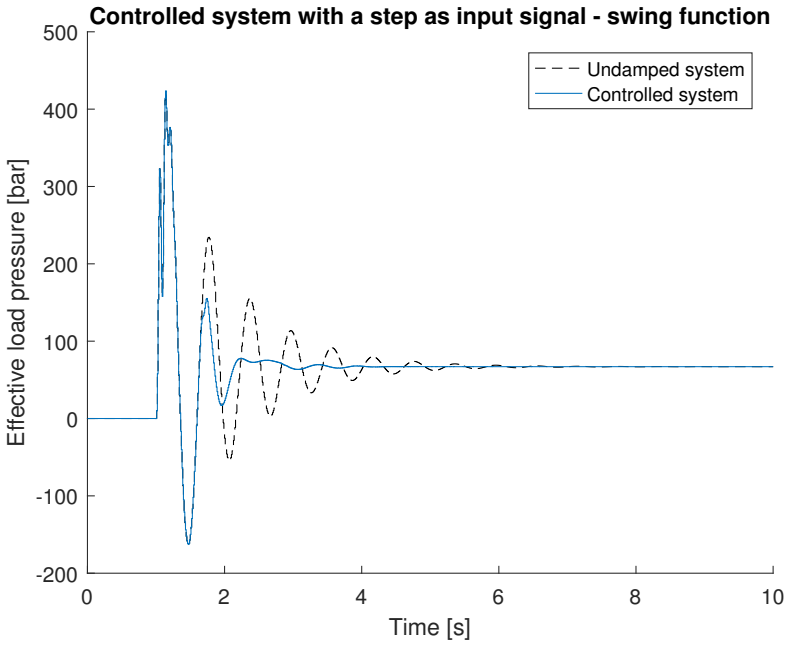

Figure 5.18: Step response of the swing function comparing the effect of the complete controller when the RLS identifier is used.

When looking at the damping effect from Figure 5.18 and the effect on the boom function in Figure 5.6 it is seen that the swing function will oscillate more and has a longer settling time than the boom function. When comparing the case with known frequency and damping in Figure 5.17 and with the identifier in Figure 5.18 the damping effect will be worse since it will take some time before the identifier has become stable. This in combination with the saturated control signal will decrease the damping effect to some degree.

To get a better understanding of the identifier for the swing function the estimated frequency and damping are displayed in Figure 5.19 and in Figure 5.20.

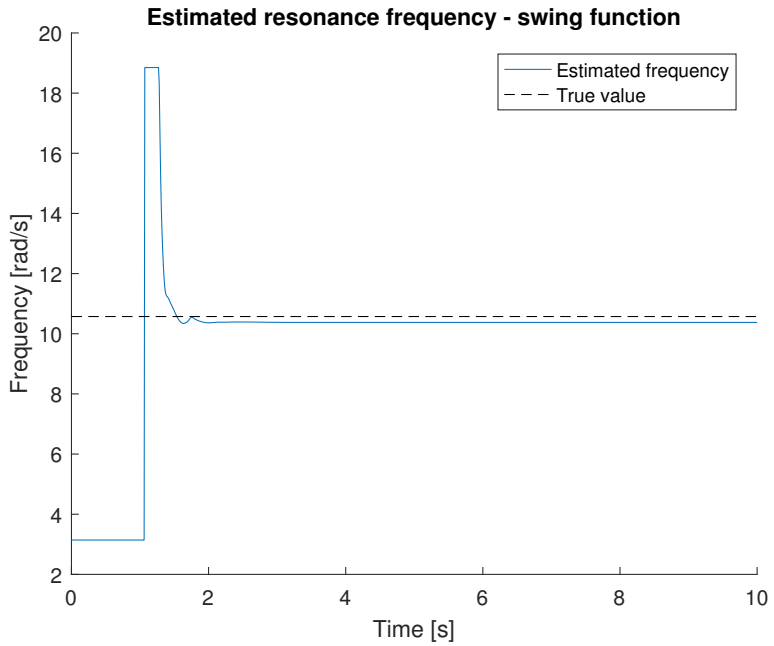

Figure 5.19: The estimated frequency where $\gamma_{max} = 1000$ and $\lambda_0 = 0.99$ for the RLS identifier. The frequency converges to ω_n=10.38 rad/s.

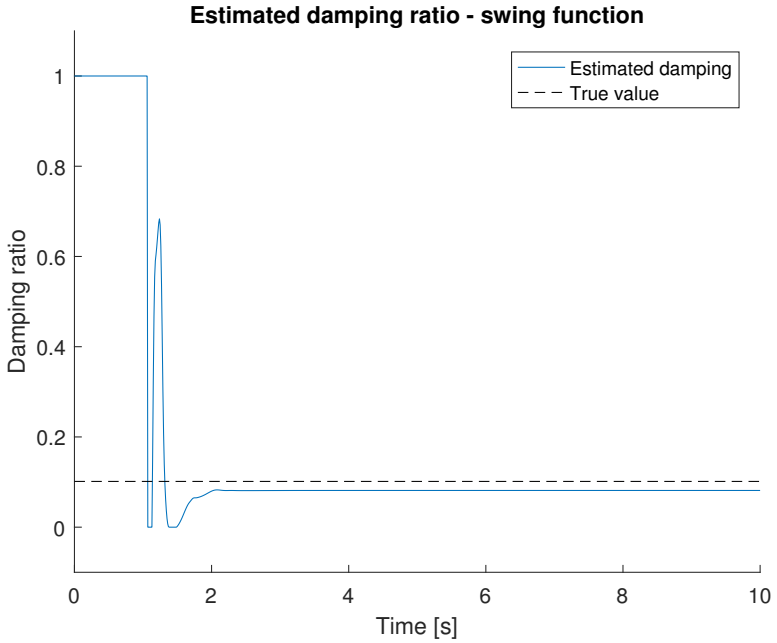

Figure 5.20: The estimated damping where $\gamma_{max} = 1000$ and $\lambda_0 = 0.99$ for the RLS identifier. The damping ratio converges to $\delta_n = 0.0813$.

The identifier for the swing function performs quickly with a settling time around 2 seconds and has a decent accuracy. The estimated frequency converges to $\omega_n = 10.38$ rad/s where the true value is $\omega_n = 10.57$rad/s and the estimated damping converges to $\delta_n = 0.0813$ and the true value is $\delta_n = 0.101$. Since the identifier is based on a simplified model of the system the estimation will only be close to the true value.

5.2.3 Simulation with the Kalman filter identifier

The swing function is also simulated with a Kalman filter as the identifier. The step response for this can be seen in Figure 5.21

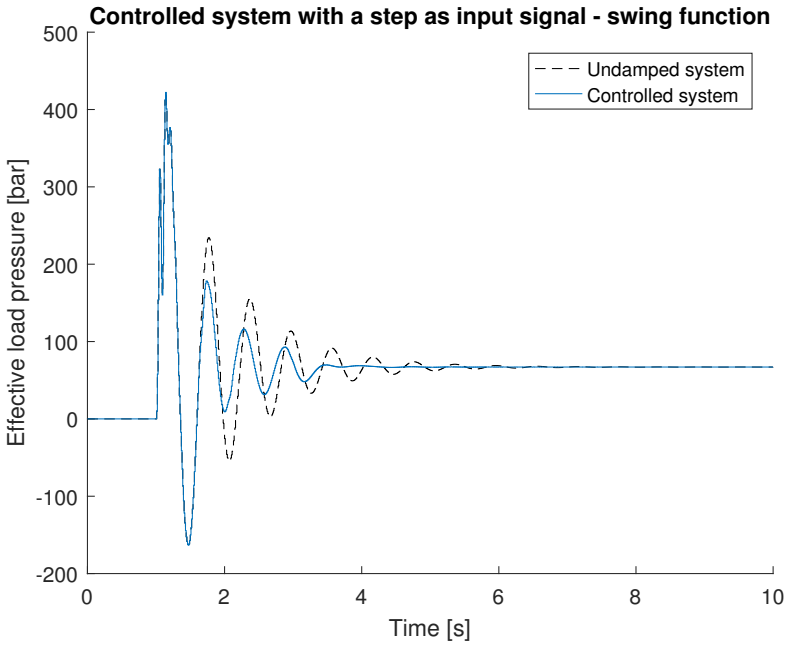

Figure 5.21: Step response of the boom function showing the effect of using a Kalman filter for the identification.

When using the Kalman filter for the swing function the damping effect is drastically reduced when comparing when the identification is done with the RLS algorithm in Figure 5.18. When comparing the results when using a Kalman filter for the boom function in Figure 5.10 the swing function performs worse. Note that the same tuning has been used as in the case of the boom function, i.e. $P = 1000$, $R = 0.99$ and $Q = 1 \cdot 10^{-3}$.

The main reason for the poor damping are the estimated resonance frequency and damping which can be seen in figure 5.22 and respectively Figure 5.23.

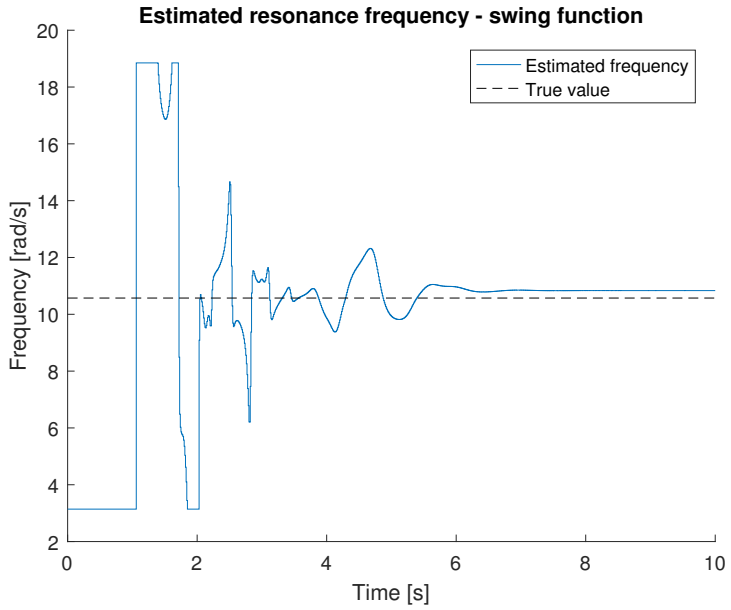

Figure 5.22: The estimated frequency where the values $R = 0.99$, $Q = 1 \cdot 10^{-3}$ and $P = 1000$ has been used for the Kalman identifier. The estimated frequency converges to $\omega_n = 10.83$ rad/s.

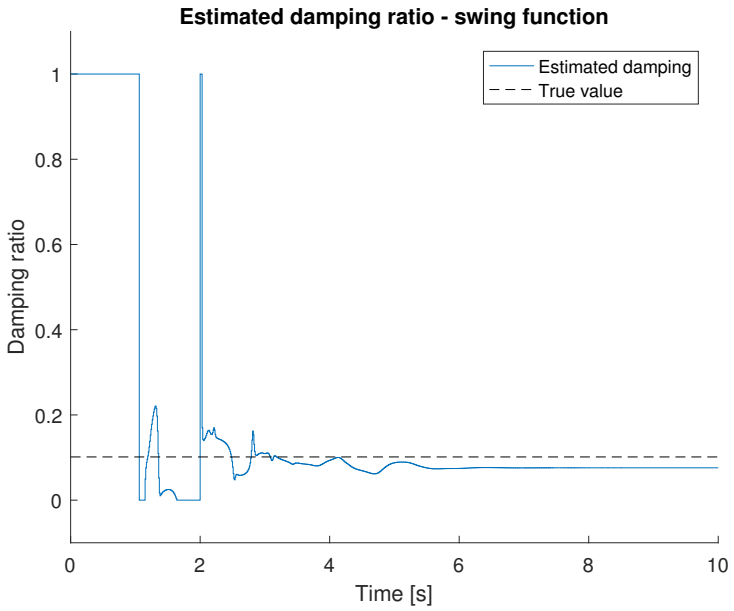

Figure 5.23: The estimated damping where the values $R = 0.99$, $Q = 1 \cdot 10^{-3}$ and $P = 1000$ has been used for the Kalman identifier. The estimated damping converges to $\delta_n = 0.0758$.

The estimated frequency has a much more aggressive convergence to the true value of $\omega_n = 10.57$ rad/s and converges to $\omega_n = 10.83$, and hence the poor damping effect. The same conclusion applies on the estimated damping which converges to $\delta_n = 0.0758$ compared to the true value of $\delta_n = 0.101$.

5.3 Simulations with different type of input signals

Until now the only input signal that has been used is the basic step. This is however not always the most realistic command signal for mobile machines, but they do give a hint of the overall system behaviour. The most common types of input signals are in the form of a ramp, since most crane operators have a more harmonic feel when they steer the joysticks. Simulations of this can be found in Appendix C for the boom function, and it confirms the good damping effect of the system when using ramp signals as input.

It can also be interesting to see how several steps of the input signal is affecting the system and how the controller copes with it. These types of simulations are also presented in Appendix C where a step up and step down signal is used as input.

5.4 Conclusions of the simulations

The main conclusion that can be drawn from these simulations are that if the frequency and the damping of the system is known, the damping will be only affected on how the user selects the feedback filter and the feedback gain. When the RLS-identifier is used the damping effect will be less, but it will be adaptive to system changes and the estimates converges quickly. The Kalman filter however, has not proven to be sufficient as an alternative to the RLS-algorithm, some modification to the Kalman filter would be needed in order to reduce the uncertainties and the slower convergence rate.

Chapter 6

Embedded Implementation of the Controller

In order to test the control algorithm in a real application an embedded implementation has been done. This was achieved by first implementing the control algorithm in Simulink and then generate code from the that model. The code is then flashed to Parker Hannifin's electrical control unit. This chapter will discuss how to implement the generated code and what was changed from the control algorithm that was used in the simulations in Chapter 5.

6.1 Electrical control unit

The electrical control unit that is offered from Parker Hannifin is a Vansco module CM3620 which has support for 36 inputs and 20 outputs [14]. The module was used as a prototyping platform for this master's thesis, and its limitations have been investigated.

The ECU is capable of controlling the two magnetic solenoids on the valve through a current PWM signal from the I/O ports. The solenoid then controls the flow to the spool which then enables it to move forward or backward. The main specification for this ECU that should be noted is that the sampling time can be set to a maximum of 100 Hz or 0.01 seconds, and the RAM size is limited to 48 kilobytes.

6.1.1 Hardware limitation

When implementing a discrete controller, one critical part is to know what the minimum sampling time is, which is needed for the control algorithm to work with the ECU, since the ECU has a limited sampling time. This is important for the dynamic pressure feedback part of the controller should work properly. Since the pressure feedback only prevents oscillations when they have arisen, the controller must therefore be fast enough to read the pressure measurements and control the solenoids simultaneously.

If the dynamics of the crane is investigated it can be noticed that the slowest frequency will be the mechanical resonance frequency, which is at most 5 Hz. This frequency corresponds to a response time of $\frac{1}{5} = 0.2 = 200$ ms and will have the dominated dynamics as previously discussed in Section 3.5.1.

One common rule of thumb in control theory is that the response of the control system must be at most one fifth of the period of the oscillations. This implies that the response of the controller would need to be at most 40 ms. The ECU-unit has 10 ms in sampling time and this should be sufficient to satisfy the sampling time criterion for resonance frequencies of 5 Hz.

6.2 IQAN

Parker Hannifin have developed aline of control system products under the name IQAN, which are used for controlling the hydraulic systems in mobile machines. The IQAN system allows the user to monitor different IQAN-units that are connected together through a CAN-network. IQAN is usually used together with Parker Hannifin's valves and other control systems in order to monitor and control the behavior of the machine it is operating on. It has the possibility to create own control scheme in a similar way with blocks as in Simulink, however, this is not used for this project since it will not allow custom algorithms. The main reason for using IQAN is the easy access communication protocol CAN, which will be discussed more thoroughly in the next subsection.

6.2.1 CAN - communication protocol

To send the generated code to the ECU a Controller Area Network (CAN) protocol is used to transmit and receive data. The generated Simulink code can be uploaded through a USB/CAN adapter and then be used by the ECU. The CAN protocol is a standard for industrial communications and it has its benefits from having low cost, priority messages, error capabilities and lightweight network [18]. The CAN protocol has primarily been used in the automotive industry but is now very popular in hydraulic systems, due to the convenient properties of the CAN protocol.

The CAN terminology can be explained as the CAN device sends data across the CAN network in packets called frames, also referred to as messages. In the CAN frame each signal is contained by 8 bits of data and each frame can contain up to 64 individual signals and 8 bytes of data for the entire frame [18].

For our system, the main signals that should be communicated with the CAN protocol is the measured pressure in service ports A and B, and the command signal from the operator. The monitored signals can be chosen differently, depending on what the user is interested in that is calculated from the controller. For this thesis, the main signals that can tell us how well the adaptive control acts are the estimated frequency, estimated damping, the control signal, and how well the effective load pressure is damped. Besides the signals that are used to monitor the performance of the controller, the CAN

communication also allows the user to send parameters to the controller for easy on-line tuning. This will be very convenient when tuning the controller on-line.

Since the CAN protocol is done in binary, each message received will be decoded into a "real world" value. This will be done by a module through Parker Hannifin's IQAN system which supports CAN [12].

6.3 Code generation

One crucial part in order to test and verify the controller on a real machine is that the control model needs to be described in a programmable language. The language will be in C since this is what the ECU supports. This is where Simulink comes in place, since it supports code generation. The built control model can be exported as code which includes all the necessary .c and .h files. The code generation tool needs information about the targeted processor from the ECU, and the model needs to be in a real data type before the generation can be done.

Before the code can be uploaded to the ECU it needs to be wrapped with some external codes which selects the right I/O for the ECU and how they should be controlled. The external code is also used when setting up the CAN protocol when deciding which signals should be in which CAN frame. This external code is created by Parker Hannifin and is made to import Simulink code in a specific way to be supported by the ECU.

6.4 Fixed-point arithmetic

Since the Simulink model uses floating-point arithmetic, the model needs to be converted to fixed-point arithmetic in order to work with the ECU's processor. This can be done with the help of MATLABS's fixed-point designer tool [23]. This tool can automatically select a fraction length for each variable for a given word length, and rounding method for the model that needs to be in fixed-point.

The main benefits when using fixed-point representation is that the computation cost will be lower than using floating point, hence less CPU power is needed. The drawback is that there can be an increase in development time, and problem with the resolution of the result. The resolution of the fixed-point representation is limited to the word length, which decides how big the range of the numbers can be. The fraction length in fixed-point tells us how the numbers will be sacaled For this thesis the ECU has a 16 bit processor and the word length will be limited to 16 bits, meaning that there is an maximum of $(2^{16}) - 1$ bits to use for number representation, for a desired range together with the fraction length.

Some algorithm can be complicated to convert, and simulation and validation needs to be repeated in order to reduce the error relative the floating-point version.

6.4.1 Delta parametrization

Since the model will be described in fixed-point arithmetic, there can be problems with quantization errors when using the regular shift operator z^{-1}. In order to avoid unnecessary errors the delta parametrization is used, which changes the shift operator to $\delta = (1 - z^{-1})$ [16].

6.4.2 Filter performance

Due to the discrete filters used in the controller, certain modifications are needed in order to be applicable to the fixed-point representation. For instance, the band-pass filter of second and third order needs to be cascaded at least to a second order transfer function in series. By doing this the filter will have simpler integer coefficients, reducing the error with fixed-point [4]. This means that the filters will have to be redesigned. For the second order band-pass filter it is implemented by first use the low-pass part, and then the high-pass part.

Since the filters are described recursively, i.e. infinite impulse response filters (IIR), there can be difficulties when using fixed-point representation. When using filters in fixed-point arithmetic, finite impulse response filters (FIR) are easier to implement, since they are often designed with fixed break frequencies and does not need to be computed recursively. The break frequencies need to be able to vary over time and therefore this is not an option to use. Therefore, the IIR-filters will be used and the filter equations needs to be converted to fixed-point with care and compared with its floating point representation, in order to reduce the errors.

6.4.3 Performance of the control algorithm in fixed-point

The control algorithm has shown to be difficult to fully implement in fixed-point representation. The main part of the controller that has not shown to work is the identifier, i.e. the RLS-algorithm, meaning that there are errors between the floating-point and fixed-point model in Simulink, such as overflows and instability. The reason seems to be numerical instability with a limited range with matrix multiplication and the recursive equations that the RLS-algorithm contains.

This has led to that the identifier is not included in the embedded version of the controller, making the solution not adaptive, and the resonance frequency and the damping of the system will have to be selected as tuning parameters.

6.5 Current control for the magnetic solenoids

The suggested controller creates a control signal that goes from -100% to 100%. However, this signal needs to be translated to a unit that is supported by the solenoids on the valve. They operate in the span of 0-1000 mA and can be controlled with a PWM signal from the ECU. The control signal has to be

linearly scaled to the current and then to the corresponding duty cycle for the PWM signal. Depending on which sign that is sent from the joystick signal, different solenoids are controlled, e.g. 100% command signal will generate the maximum current that is the sent as a PWM signal to the solenoid which makes the crane move up. This must be implemented in code to select which solenoid to control for a given input signal from the joystick.

However, since the solenoids control the flow of the fluid, there will be a reactive force on the magnetic actuators. There will also be a temperature disturbance due to hot oil, which will cause the solenoids not to move the spool as intended. This is commonly solved by using current control, i.e using feedback of the low sided current from the magnetic actuators. The feedback current is then used with a PI controller with feed forward control of the set-point, in order to minimize the hysteresis.

6.5.1 Dead-band compensation

As discussed in Section 2.2, the valve has dead-band characteristics, which needs to be compensated for in order to get a smooth control for the operator. This is commonly done by setting the minimum and maximum current for the solenoid, i.e. choosing the minimum current which will cause the spool to start moving and the maximum current for the spool's speed. This is then linearly scaled for the control signal. The minimum and maximum current will depend on what type of spool that is inside the valve and on the solenoids. This means that each solenoid needs to be tuned separately, since they will not always have the same minimum and maximum currents. For the L90LS valve the minimum current is commonly around 260 mA, and the maximum is commonly around 510 mA [11].

This problem can also be solved by linearizing the valve, i.e. use the inverse characteristics of the valve to cancel out the dead-band, this is done in [20], and also suggested in [22].

6.6 The final embedded controller

The final embedded controller can now be constructed and for illustrative purpose the basic concept is seen in the block diagram in Figure 6.1. Everything in the block diagram is implemented in Simulink, converted to fixed-point, exported to code, and wrapped together with the external code.

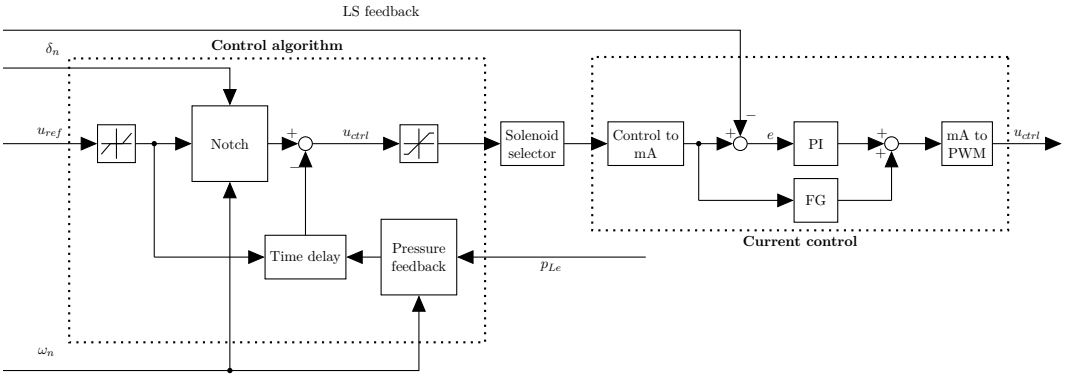

Figure 6.1: The complete control system in the form of a block diagram where the inputs are u_{ref}, δ_n, ω_n, P_{Le}, and LS

The input signals for this controller are the tuning parameters for the dynamic pressure feedback, the command signal u_{ref} from the operator, the effective load pressure p_{Le}, the damping for the system δ_n, the resonance frequency ω_n, and the low-side current LS for the current control of the solenoids. Note that a dead-band of 10 % is used on the command signal to lower the sensitivity on the joystick. The solenoid selector selects and sends the control signal to the solenoid that should be actuated. The control to mA scales the control signal to minimum and maximum current for each solenoid.

Chapter 7

Experiments and Results

This chapter will cover the executed experiments in lab environment and in the mobile machine, the forwarder. The chapter will be ended by presenting the results from the experiments, which is only tested for the boom function. The cylinder of the boom function has been of the single acting type, meaning that only pressure is applied to service port A, which is not the case for the derived model in Chapter 3 that is of double acting type. It should also be noted that all experiments are done without the identifier part of the controller due to the hardware implementation problem.

7.1 Preparation

Before the experiments can be carried out in a lab environment, the embedded controller needs to be calibrated/tuned with the valve it should be operated on. This will be done by choosing good parameters for the P- and I-part for the PI-controller for the magnetic coils and the feed-forward gains. Since the valve L90LS may have different properties depending on its current specification, different valves may have to be tuned individually. The maximum and minimum current will also be needed to be tuned as stated in Section 6.5, and they were found to be roughly around 280 mA to 500 mA for both solenoids.

7.2 Experiments on the L90LS in lab environment

Before the control solution can be used on a real crane, some testing and verification needs to be done in a closed lab environment. The lab was supported with an L90LS valve and the ability to control the flow, and pressure from the pump to the A and B ports. A single acting boom function was implemented on the valve which meant that there is only flow going to port A of the valve.

Since the testing is done directly on the valve, the main oscillatory characteristics are very small, and nearly none-existing. This is because there is no external mass and arm that can oscillate as in on a real crane. Therefore, the damping effect will be hard to distinguish when comparing with the case

when the controller is not used.

However, the experiments in the lab shows how responsive the controller is and that it is capable of controlling and reading the values from the pressure sensors without any delay. Figure 7.1 displays the lab experiment of a step response from -100% to 100% of the command signal, for the cases when the controller is active and not active.

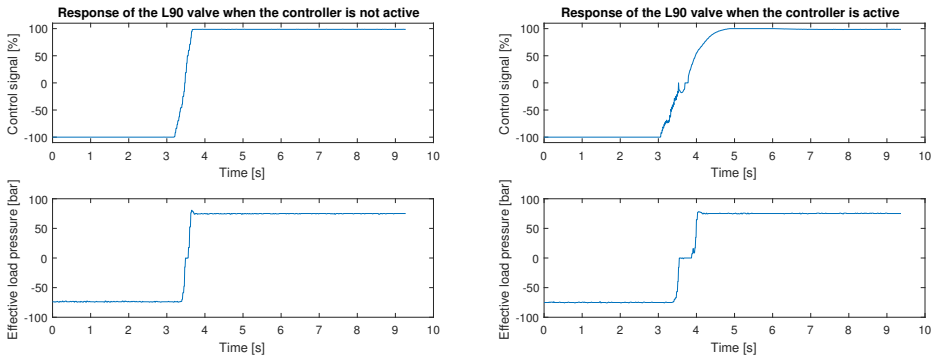

Figure 7.1: Figures from the lab experiment showing the effective load pressure with the control signal when the controller is active and not active.

It can be seen in this experiment that there are not any large oscillations that occur since the valve by itself is rather stiff. However, the controller manages to dampen the small pressure spike that occurs at 4 seconds which is about 3 bar. It can also be noted that the pressure will have a larger dead-band behaviour when the controller is used, due to that the notch filter of the controller will act immediately when the control signal enters and leaves the controller's dead-band. This means that when the control signal is zero, the valve will be closed. It should also be noted that in the lab experiment the pump pressure is constant, which is not the case in real mobile machine that has variable pump pressure. This is the reason for zero pressure when the control signal is zero. For this experiment the parameters for the controller are displayed in Table 7.1.

Table 7.1: Tuning parameters for the L90LS lab experiments

Parameter	Value	Description
K_{fb}	$1 \cdot 10^{-3}$	Dynamic pressure feedback gain, higher value increase the impact from the pressure change
ω_n	1 Hz	The resonance frequency
ξ_1, δ_n	0.05	The width of the notch filter/damping of the system
ξ_2	1	The depth of the notch filter
ω_{cl}	3	The lower cut-off multiplier on the resonance frequency for the band-pass filter
ω_{cu}	1/3	The upper cut-off multiplier on the resonance frequency for the band-pass filter
ξ	$\sqrt{2}/2$	The damping ratio of the band-pass filter

It should also be noted that for this experiment the resonance frequency and the width of the notch filter are not known and have been tuned to give a reasonable amount of damping effect. When the controller is implemented on a real machine, the response and the behaviour of the crane will have a significant impact when choosing the right tuning parameters for the controller.

7.3 Experiments on the crane

The machine that has been used during the experiments is a forwarder, which is used to move logs in a difficult terrain. For simplicity, the forwarder has been in a fixed position during the test, and only testing the crane's boom function. The forwarder is over 30 years old, and it has an overall low damped structure, due to the combination with big rubber wheels on hard asphalt. This makes it act like a mass spring damper system, similar to the one derived in Chapter 3. It is also important to note that the spool used in the L90LS valve does not have any hydraulic pressure feedback which can sometimes help to dampen the system passively. With this in mind the test system is very prone to high pressure peaks and oscillations, compared to a newer machine. For all of the tests the effective load pressure and the control is shown when the control algorithm is active and when it is not.

It should also be noted that for all of the experiments there is some delay between the tests, which can be seen when the control signal is compared for the different tests.

7.3.1 Tuning the controller

For the following test the controller has first been tuned in order to get some good understanding on how well it can dampen the system. This is done by testing the boom function up and down and see how much it oscillates. This will give a hint of the resonance frequency of the function, and for the boom

function it was found to be around 2 Hz. It should be noted that this way is not the most suitable method to have a fixed resonance frequency since the frequency will change depending on the length and mass of the crane. For example, 2 Hz may work for the unloaded case, but when a load is added the frequency will be different, and hence the damping effect from the controller. But for easier comparison of the test results this setting has been chosen to be constant throughout the experiments.

The other tuning parameters such as the band-pass filter cut-off ratio and damping have been set to the same values as in the simulations in Chapter 5. The pressure feedback gain will be tuned by increasing its value from 0 and upwards with a slow increment until a good damping behaviour is acquired. The most difficult parameter to set is the damping for the system; the easiest way is to tune the other parameters first and then slowly increase the damping from 0 and up. The tuning parameters for the boom function used in the experiments are listed in Appendix D.

7.3.2 The boom function

The boom function is tested with no load attached to the grapple of the crane with a step as input, which is presented in Figure 7.2. Here the boom is lifted up and then released, first used with the controller inactive, and then when it is active. It should be noted that lifting the boom up is a very smooth function and if the command signal is not aggressive on the way up. The larger oscillations will only occur when the boom is released, causing the grapple to start oscillating since it can swing freely. This can be seen in the Figure 7.2 after 4 seconds. The small pressure dimples at the beginning from 2 seconds to 4 seconds are caused by the arm of the crane is flexing, or also referred to as deformation. The main vibration that is felt in the forwarder, and that will cause the most trouble, is when the function is released, i.e. the oscillations at 4 seconds.

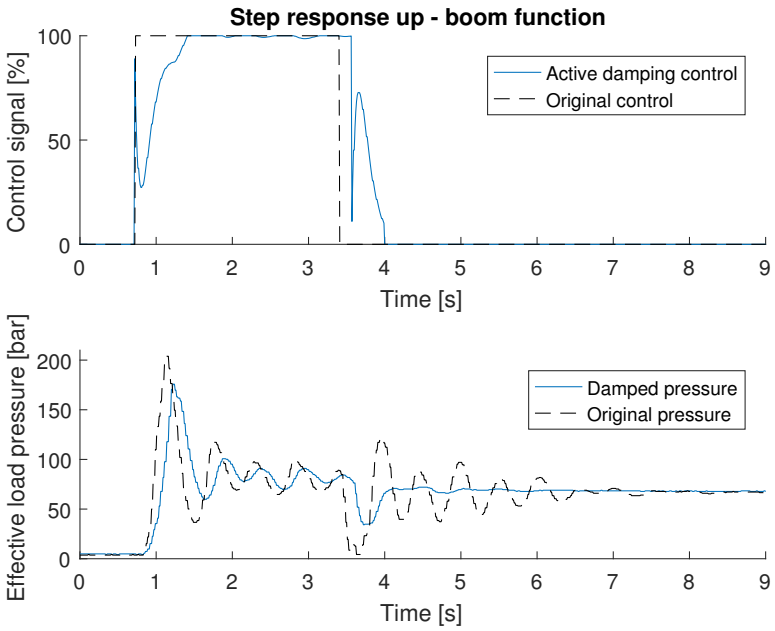

Figure 7.2: Step response up of the boom function with no load.

When testing the opposite direction of the boom function, i.e. a step down, the damping effect will be higher with the controller is active. The result will get a bit more aggressive depending on how fast the crane arm is dropped, since the crane will have the gravity in the same direction which helps to accelerate it. It will also oscillate more frequently due to the grapple can swing freely. The step response down test of the boom function can be seen in Figure 7.3.

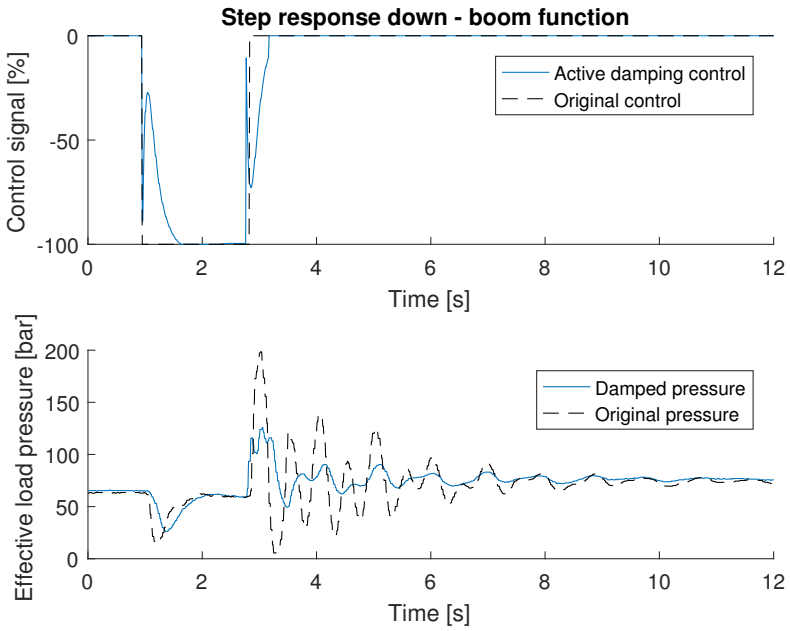

Figure 7.3: Step response down of the boom function with no load.

When the step up and step down are used together the machine gets exposed to even more pressure changes which is seen in Figure 7.4. When the crane is influenced by more movements after each other the crane will be influenced by high pressure spikes, which is seen for the undamped cases. The controller manages to suppress those spikes which results in a smoother behaviour of the crane.

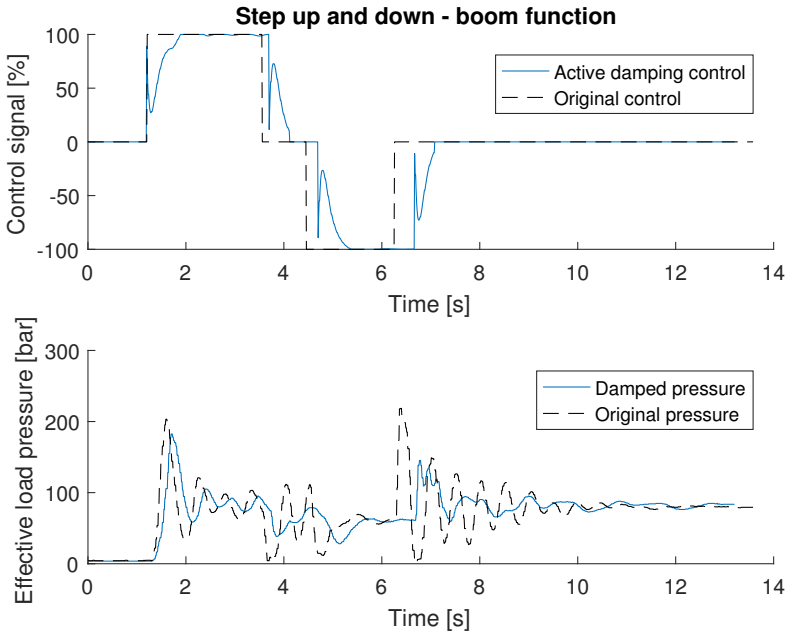

Figure 7.4: Step up and then step down of the boom function with no load.

One other thing to test is the effect of the notch filter. As for the previous experiment the main damping effect will come from the dynamic pressure feedback, the notch filter can only dampen oscillations induced from the command signal. The effect of the notch filter can be tested by shaking the joystick controller rapidly up and down. The undamped case will not restrict these command signals, which will cause a very uncontrolled behaviour of the crane and on the whole machine. This is not something that is usually done by the operators, instead they use more controlled and slower movements on the joysticks, due to oscillations. Figure 7.5 displays how the controller dampens this behaviour, which proves that it can handle more aggressive joystick movement.

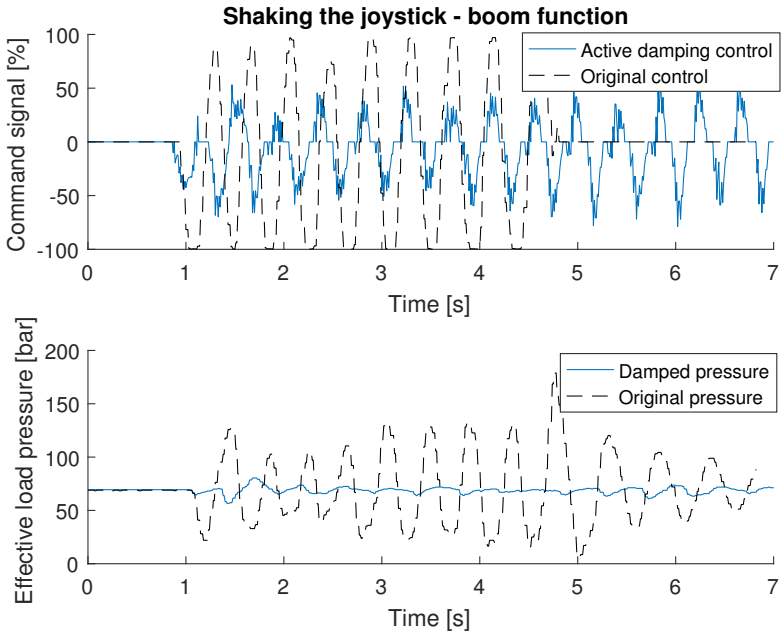

Figure 7.5: Shaking the joystick up and down, creating an oscillating behaviour of the boom function.

When it comes to robustness of the controller it will have some problems when there is a change of system parameters, such as an increased mass or length. This has been tested by increasing the crane's arm length and using the same tuning parameters for the case when the crane is not fully extended, seen in Figure 7.6. Even though the resonance frequency of the system changes, the controller manages to dampen the oscillations to some degree. When the mass is increase the resonance frequency will be lower, as shown in Table 3.1, the same conclusion holds when the length is increased instead. Therefore, the damping can be improved by lowering the resonance frequency parameter for the controller. This has been done by setting the resonance frequency to 1.7 Hz and compared to when it is 2 Hz, which is seen in Figure 7.7. There is a small difference between the two cases, when using a lower frequency, the pressure spikes will be even more damped, making the controller much more prone to stop the oscillations after the command signal is in neutral position. But it should be noted that if the frequency is changed to 1.7 Hz for the case when the arm is not extended, will be worse then at 2 Hz. This is the main concern when the identifier part is not used, since the resonance frequency will change constantly.

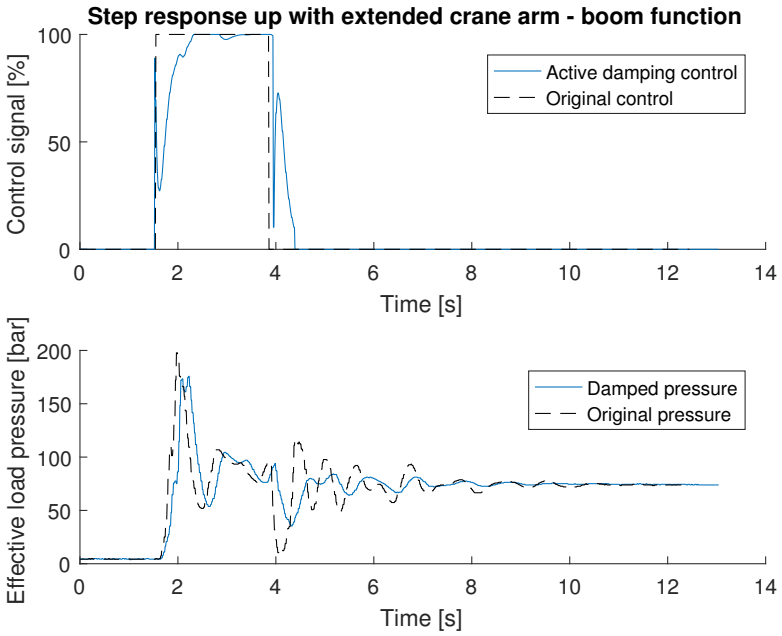

Figure 7.6: Step response up of the boom function with the arm fully extended.

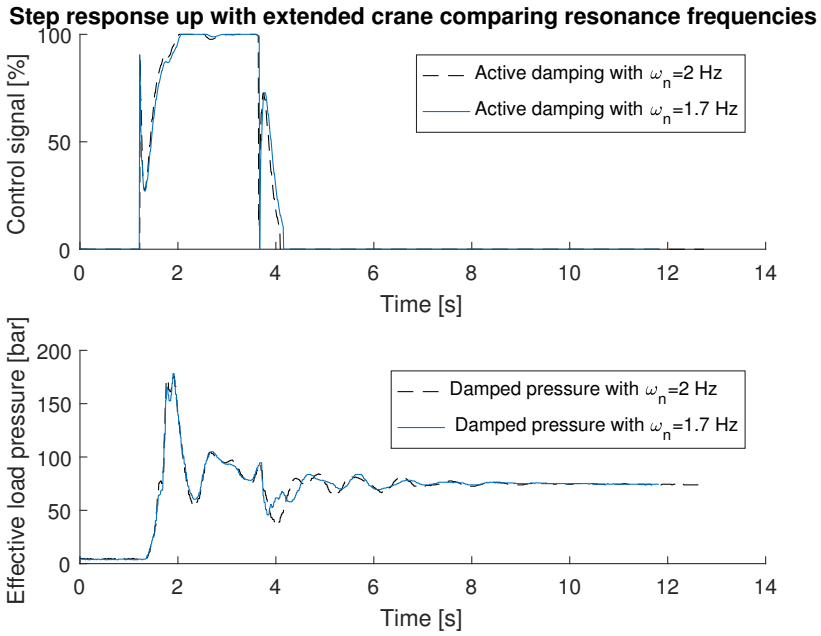

Figure 7.7: Step response up of the boom function with the arm fully extended, comparing change of resonance frequency.

All the above experiments indicate that the control solution can dampen the oscillations when using the boom function, and roughly estimated to suppress the pressure oscillations by 30-50% by looking at the results. However, if the system parameters are changed like the length of the crane arm, i.e. using the extension function, the result will be different. The same reasoning applies if the crane is lifting a load. Since the identifier cannot be used in the experiments, these tests will be needed a separate tuning from the ones used for the first experiments, in order receive the most damping effect.

In Appendix E the experiments of using the crane with an applied load are shown, and also how changing the frequency increase the damping effect. Those tests indicate that even if the controller is not adaptive, it is still robust enough to dampen the high pressure spikes. For different system changes, it will still need some tuning in order to get out most of the active damping.

Chapter 8

Conclusion

This chapter will go through the outcome of this project, and discuss its relevance. It will also include some reflections regarding the presented research questions that were stated in Chapter 1.

8.1 The simulations

The simulations that were presented in Chapter 5 indicates that the complete control solution can dampen the pressure oscillations drastically. They also show the importance of identifying the resonance frequency quickly in order for the solution to be stable, and give sufficient amount of damping to the system. The derived model for the system is simplified, although, the model used for the identifier is even simpler and dose not include the dynamics from the valve and hydraulics. This creates a small error for the estimations, however, there will still be a moderate damping effect when the active damping controller is used in simulations.

8.2 The controller

The main concern is that the embedded solution is not adaptive due to implementation problems with the hardware. As stated in the scope and boundaries in Section 1.4 the control unit needs to be able to do all the necessary calculations, (iii). Regarding this statement, the current solution with a fixed-point processor has numerical difficulties.

This resulted in that the identification part could not be implemented in the embedded software. Instead the mechanical resonance frequency, and the damping of the system, must be chosen for each function and this is not ideal, since the mobile machines have a varying system dynamics.

8.2.1 The identifier with RLS

The problem with the implementation of the identifier is the numerical instability when converting the algorithm to fixed-point arithmetic. The numerical

instability of the RLS algorithm is said to be an issue when there are round-off errors, causing the precision of the covariance matrix $P(t)$ to be poor and the positive definiteness is lost. One solution to this problem is to implement a square-root algorithm to propagate the square root of the covariance $P(t)$, that is $P(t)^{1/2}$, such as $P(t)^{1/2}P(t)^{T/2} = P(t)$. This method might solve the numerical problems that are caused by the fixed-point implementation [24].

8.3 The embedded implementation

One of the goals for this thesis was to see how an adaptive controller could be implemented as an embedded software, and used with commercial products that are currently on the market. This has been tested and validated to work for some algorithms and filters. However, as already pointed out, some algorithms are more difficult to implement due to numerical complexity and therefore require more processing power to be fully implemented. The outcome of this thesis has shown that IIR-filters, PI-controllers, and logic can be implemented with a 16 bit-processor with fixed-point arithmetic and give the same resolution as the floating-point arithmetic.

It should be noted that it is not ideal to work with complex algorithms and many customized recursive equations in fixed-point, as it can cause errors and long development time. It has been the most time-consuming part of this thesis, to structure every equation and variables that is used in the MATLAB/Simulink code in order to generate an equal structure in the C-code for the embedded processor.

8.4 Performance of the controller in experiments

The performance of the controller, as seen in the Chapter 7, indicates that the suggested control algorithm can dampen the system sufficiently if it is tuned properly. This can also be felt in the cabin where the pressure oscillations will have a smaller impact on the entire machine. For the boom function the most oscillations occur when the crane is stepped down fast and it is much more controlled when stepping up the boom. Experiments also show how the command signal can be more aggressive, which implies that the system can be steered much faster without any high pressure spikes affecting the overall system. A major concern with this type of control solution is that, the time delay as mentioned in section 4.3, will make the controller only dampen oscillations when the control signal is active. This will make the controller not to dampen out the oscillations when the crane movements have stopped. The controller can still dampen those types of oscillations but only if the pressure oscillations are sufficiently damped before the joystick is left in neutral.

If the arm is extended or a load is added the high pressure spikes will be damped but some of the oscillations might still occur since the grapple starts to swing immediately when a movement is stopped.

8.5 Final comments on the thesis outcome

The first aim of this thesis, presented in Section 1.2, was to implement active damping for an embedded application in hydraulic valves. This has not been fully fulfilled. The solution works in simulations but for the implementation on the forwarder the solution is not adaptive to changes in the mechanical resonance frequency and the damping of the system. The second aim was to evaluate the performance of the solution and analyze its limitations. Regarding this point the importance of the processing capabilities of the ECU and the development time with fixed-point arithmetic on the current system can be concluded.

In the introduction in Chapter 1 several research questions were stated, and all has been investigated throughout the project.

RQ-1 What types of models are needed for testing and validating a control strategy?

When it comes to the derived model it has shown how oscillations in mobile systems can appear and behave, hence it gives some answers to research question RQ-1.

RQ-2 For a hydraulic valve system, what control strategies are suitable to use?

For the suggested control algorithm, it was shown to be easy to setup and simulate together with the model of the crane. Therefore, a suitable control strategy is to filter the input signals with the damping of the system and with the resonance frequency, and feedback the pressure with the same frequency.

RQ-3 How can robustness be achieved by applying active dampening to hydraulic systems?

The final research question that has been investigated is somewhat hard to give a straight answer to. The adaptive control solution works in simulations and it proves that the control algorithm can be robust to different system changes. However, the suggested embedded implementation for the problem is not adaptive, and hence it will not be robust in different hydraulic systems. If the control solution is tuned with the right amount of feedback gain, a chosen resonance frequency and a chosen damping of the system it can dampen the system in a controlled way without the identification part. More tests will be needed in order to clarify if the simplified control solution can be robust in different systems with different parameters. For instance, testing the machine by a well-trained operator in a suitable environment, which will push the control solution to its limits.

Chapter 9

Future Work

This chapter will present what can be improved from the thesis in future implementations. This regards the mathematical model, the control algorithm, embedded implementation, and the experiments.

9.1 The mathematical model

One major part of the mathematical model that can be improved is to model the valve input in more detail. The model can at the moment accept any input as valve input as long as it has a relationship to the spool position. In the experiments, the valve input was a joystick input from -100% to 100% which then was connected to the two respective solenoids. These solenoids could be modelled as a joystick input to a desired current output, and included in model. Methods on how to model solenoids have been done in [5]. This could be interesting to analyze the effect of the solenoids when using the model of the crane.

One thing that has been excluded from the original model, derived in Chapter 3, is a transfer function describing the valve input to load position, included in [9]. This was excluded due to the lack of position sensors, hence no comparable references for experiments could be calculated. However, it could become interesting to include the load position in future development of the model as the trend of the hydraulic industry is focusing more on load positioning control and the use of sensors on cranes.

9.2 The fixed-point representation of the complete controller

Simulations shows that the controller can be robust in hydraulic systems if the RLS identifier is used. Therefore, more time needs to be spent on the conversion from floating-point to fixed-point for the RLS-algorithm. As mentioned in Chapter 8, a different approach on the implementation of the RLS-algorithm needs to be conducted in order to make the embedded control solution adap-

tive. If it is not possible to implement the RLS-algorithm on the ECU, then some form of look-up table could be useful. Which means that depending on which functions that are in use, different values of the damping and the resonance frequency is selected from the look-up table. However, it could require many tests in order to find good values for different combinations.

9.3 Evaluation on different hardware

Processors that only support fixed-point arithmetic are commonly used in the industry, especially in signal processing with digital signal processor (DSP) for filtering and controlling. However, the increased need of processing power computer science, and in other engineering fields, have increased the usage of floating point processors, and they are now commonly used for embedded software.

Therefore, it would be interesting to test the adaptive controller on a processor that supports floating point. This could lower the development time when debugging and testing different algorithms, hence reducing the total development cost.

9.4 Evaluation on different mobile machines

For the experiments, the active damping was only tested on one forwarder, which was one of the oldest at that test site. It would be interesting to see how the active damping solution would behave on a newer system, which has a better overall damped structure. For the experiments, the forwarder was placed in a fixed position and reducing any effect of oscillations occurring while the machines moves, or is standing on a hill. This would also be interesting to do more test on, and see how well the controller works.

9.5 Adaptive controller with coupled functions

This master's thesis has only tested boom function in the experiments. Experiments on the swing and jib function also needs to be tested in order to conclude if the suggested control solution works for those types of functions. It should be stated that the main difference between the different functions are the resonance frequency; the swing function will often have a lower resonance frequency than the boom function, and the jib function will have a higher frequency. The implication is that the pressure oscillation will just change in amplitude and in frequency. Therefore, the active damping should also take care of these functions.

One additional interest lies in applying the control solution to several functions and see how well it can handle the swing, boom and jib at the same time, and investigate its performance. Questions regarding this could be:

- How will the estimated frequency behave when several functions are in use?
- Will the computational capacity of the ECU be enough to drive the adaptive controller for all of the desired functions?
- How will the damping effect behave for the complete system?

9.6 Alternative methods for controlling hydraulic valves

When it comes to adaptive control theory the literature suggest several methods that have been proven to give good results, e.g. [1]. One alternative to the adaptive solution implemented in this thesis would be to investigate how a model reference adaptive system (MRAS), could be used in order to get a better result and/or easier implementation process. The main benefits from the MRAS approach would be that the system could adapt to a desired reference which is designed by the user. This would enable more hands-on design parameters such as choosing the maximum allowed overshoot, and dead-time compared to the adaptive solution were some of the tuning parameters are hard to grasp.

There has also been research in anti-sway control for hydraulic cranes, which could be interesting to use together with the control solution in order to reduce the oscillations from the grapple after the crane function is released [19].

Bibliography

[1] Karl Johan Astrom and Bjorn Wittenmark. *Adaptive Control*. 2nd. Boston, MA, USA: Addison-Wesley Longman Publishing Co., Inc., 1994. ISBN: 0201558661.

[2] Mikael Axin. *Fluid Power Systems for Mobile Applications : with a Focus on Energy Efficiency and Dynamic Characteristics*. 2013.

[3] Mikael Axin. "Mobile Working Hydraulic System Dynamics". PhD thesis. Linköping University, Faculty of Science & Engineering, 2015, p. 85.

[4] John Thompson Bernad Mulgre Peter Grant. *Digital Signal Processing concepts and application*. Second Edition. Palvgrave Macmillan, 2003.

[5] Alessandro Dell'Amico, Magnus Sethson, and Jan-Ove Palmberg. "Modeling, Simulation and Experimental Verification of a Solenoid Pressure Control Valve". In: *:* 2009.

[6] Svante Gunnarsson and Petter Krus. "Adaptive Control of a Hydraulic Crane using On-Line Identification". In: *Proceedings of the Third Scandinavian International Conference on Fluid Power :* vol. 2. 1993, pp. 363–388.

[7] Svante Gunnarsson and Petter Krus. "Adaptive Control of Hydraulic Actuators with Flexible Mechanical Loads". In: *Proceedings of the 9th International Symposium on Fluid Power :* 1990, pp. 149–158.

[8] Svante Gunnarsson and Petter Krus. *Fluid Power Control of a Flexible Mechanical Structure*. Tech. rep. 1961. Linköping University, Engineering Mechanics, 1997, p. 36.

[9] Svante Gunnarsson and Petter Krus. *Modelling of a Flexible Mechanical System Containing Hydraulic Actuators*. Tech. rep. 1078. Linköping University, Fluid and Mechatronic Systems, 1990, p. 21.

[10] Parker Hannifin. *CAST IRON PUMPS – PGP365 SERIES*. URL: `http://ph.parker.com/us/en/cast-iron-bushing-pumps-model-365` (visited on 05/08/2017).

[11] Parker Hannifin. *Directional Control Valve L90LS*. Catalogue HY17-8504/UK. May 2007.

[12] Parker Hannifin. *MASTER CONTROLLER - IQAN-MC2*. URL: http://ph.parker.com/us/en/iqan-mc2-master-controllers (visited on 05/08/2017).

[13] Parker Hannifin. *MINI ANALOG, HALL-EFFECT JOYSTICK - IQAN-LC6-X05*. URL: http://ph.parker.com/us/17616/en/iqan-lc6-x05-analog-joysticks (visited on 05/08/2017).

[14] Parker Hannifin. *Semi-Custom Controller Module, CM3620*. URL: http://ph.parker.com/us/17616/en/cm3620-controller-modules-semi-custom (visited on 04/24/2017).

[15] Parker Hannifin. "Unpublished internal drawing of L90LS valve". 2017.

[16] P. T. Harju, J. Kauraniemi, and S. J. Ovaska. "Magnitude response optimization of delta operator filters". In: *Signal Processing, 1996., 3rd International Conference on*. Vol. 1. Oct. 1996, 83–86 vol.1. DOI: 10.1109/ICSIGP.1996.566978.

[17] H.E.Merrit. *Hydraulic control systems*. John Wiley & Sons, 1967.

[18] National Instruments. *Controller Area Network (CAN) Overview*. Aug 01, 2014. URL: http://www.ni.com/white-paper/2732/en/ (visited on 03/14/2017).

[19] Jouko Kalmari. *Nonlinear Model Predictive Control of a Hydraulic Forestry Crane; Hydraulisen metsäkonenosturin malliprediktiivinen säätö*. en. G5 Artikkeliväitöskirja. 2015. URL: http://urn.fi/URN:ISBN:978-952-60-6325-6.

[20] Marcus Larsson. "Evaluation and implementation of the active oscillation damper CADO". MA thesis. SE-581 83 Linköping, Sweden: Linköping University, 2006.

[21] Jim Ledwidge. "System Identification Parameter Estimation of a Motorcycle Suspension System". MA thesis. Dublin City University, 1995.

[22] Song Liu and Bin Yao. "Programmable valves: a solution to bypass deadband problem of electro-hydraulic systems". In: *Proceedings of the 2004 American Control Conference*. Vol. 5. June 2004, 4438–4443 vol.5.

[23] MathWorks. *Fixed-Point Tool*. URL: https://se.mathworks.com/help/fixedpoint/ug/overview-of-the-fixed-point-tool.html#brmaxnq (visited on 02/28/2017).

[24] Bernard Widrow Simon Haykin. *Least-Mean-Square Adaptive Filters*. John Wiley Sons, 2003.

[25] *Hydraulic and pneumatic equipment - Symbols for fluid diagrams*. Standard. Swedish Standards Institute, Feb. 1969.

[26] John Watton. *Fundamentals of Fluid Power Control*. Cambridge University Press, 2009. ISBN: 978-0-521-76250-2.

[27] Bo Egardt Torsten Wik. *Nonlinear and Adaptive Control - Supplement.* Department of Signals and Systems Chalmers University of Technology. Aug. 2016.

Appendix A

Parameters for the simulations

The following table displays the parameters that was used for the simulations. They are the same parameters that are used in [9].

Parameter	**Value**	**Unit**
l - piston length	0.6	[m]
d - cylinder diameter	0.06	[m]
d_2 - piston diameter	0.0416	[m]
A_1 - cross section area chamber one ($\frac{d^2\pi}{4}$)	$2.83{\cdot}10^{-3}$	[m^2]
A_2 - cross section area chamber one ($\frac{d_2^2\pi}{4}$)	$1.36{\cdot}10^{-3}$	[m^2]
B_p - friction coefficient	$2{\cdot}10^{4}$	[Ns/m]
β - bulk modulus	$1{\cdot}10^{9}$	[N/m^2]
C_1 - capacitance chamber one ($\frac{A_1 l}{2\beta}$)	$0.85{\cdot}10^{-12}$	[m^5/N]
C_2 - capacitance chamber two ($\frac{A_2 l}{2\beta}$)	$0.41{\cdot}10^{-12}$	[m^5/N]
C_{Le} - effective capacitance	$0.57{\cdot}10^{-12}$	[m^5/N]
K_c - flow pressure coefficient	$1{\cdot}10^{-11}$	[m^5/Ns]
K_q - flow gain	$1{\cdot}10^{-2}$	[m^2/s]
M_1 - mass	$2{\cdot}10^{3}$	[kg]
M_2 - mass	$12{\cdot}10^{3}$	[kg]
K - stiffness	$1.728{\cdot}10^{6}$	[N/m]
B - damping friction	$2.4{\cdot}10^{3}$	[Ns/m]
ω_v - resonance frequency for the valve	60	[rad/s]
δ_v - damping	0.5	–

Table A.1: Table over the parameters used in the simulation in Chapter 5.

Appendix B

High-pass filter in the pressure feedback

Instead of using a band-pass filter a high-pass filter is used instead as suggested in [20] the bode plot in Figure B.1 shows how the first order high-pass filter dampens the mechanical resonance frequency but increase the hydraulic frequency a bit. The effect of this is then presented as a step response of the complete system in Figure B.3. For the high-pass filter the break frequency were set to the half of the resonance frequency and the feedback gain $K_{fb} = 1 \cdot 10^{-3}$. Even though the first order high-pass filter seems to handle the oscillations it will have some problems when the input signal is changing and when additional disturbance is added to the systems. This is due to the poor damping effect that the high-pass filter gives to the pressure feedback which can be seen in Figure B.2. One remark is that the control signal has not been saturated in this result and therefore they should be compared to the unsaturated figures in the simulations in Chapter 5.

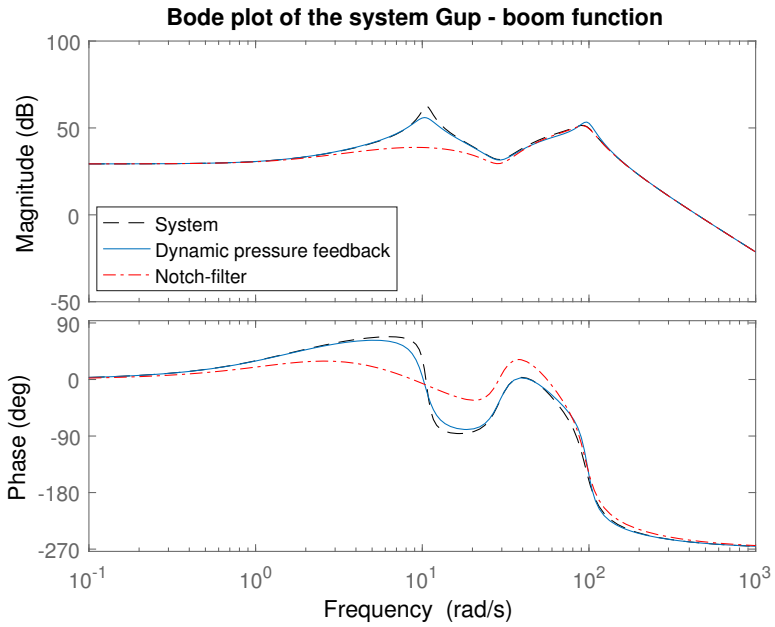

Figure B.1: Bode plot of the boom function comparing the damping effect form the notch-filter with the pressure feedback when using a high-pass filter.

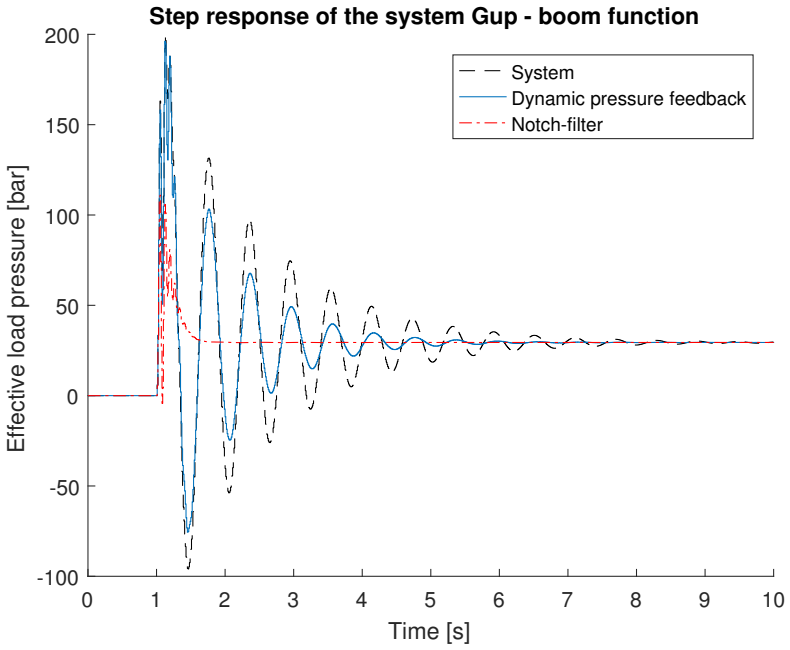

Figure B.2: Step response of the boom function comparing the damping effect form the notch-filter with the pressure feedback when using a high-pass filter.

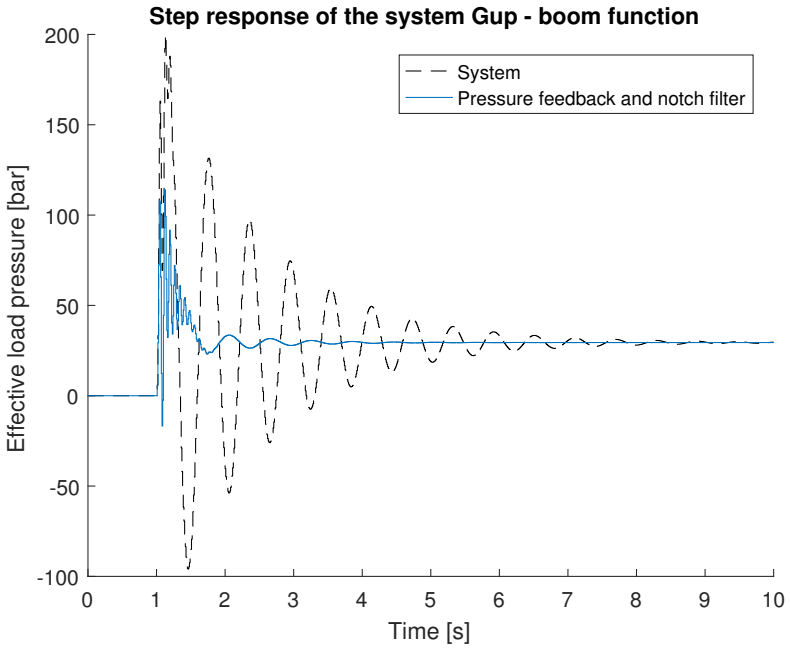

Figure B.3: Step response of the boom function comparing the effect of the complete control setup with a first order high-pass filter in the pressure feedback

Appendix C

Simulations with different types of input signals

This appendix presents additional simulations for the boom function where a step up and step down signal are displayed and also a ramped signal. In Figure C.1 a step up and step down is used form the boom function and the system gets a rather good damping behaviour. In Figure C.2 a ramp signal is instead used in order to get a more slower and smoother response from the system. It can be noted that the amplitude of the effective load pressure is much small when the systems isn't affected by rapid movements. This is one of the solution today that was discussed in the Section 1.5.2, that ramped signal can decrease the oscillation, but it will also create a slower system response.

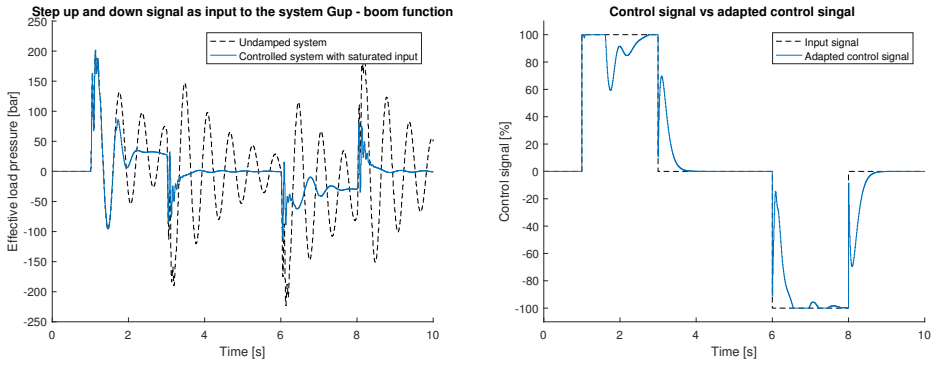

Figure C.1: Figures over the controlled system with the a step up and step down as input signal and the corresponding adapted control signal

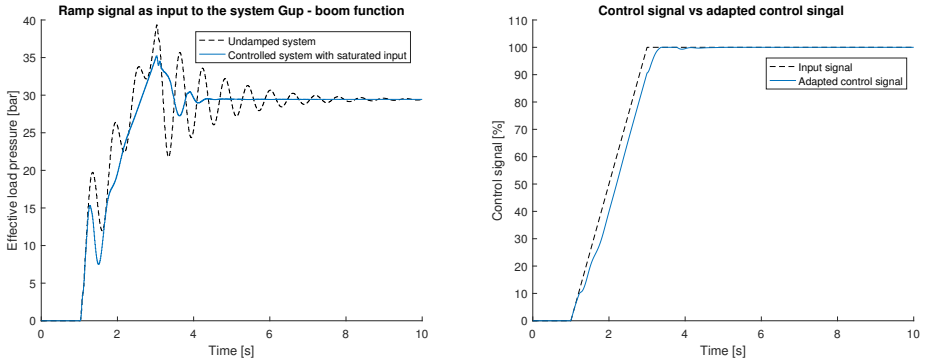

Figure C.2: Figures over the controlled system with the a ramp as input signal and the corresponding adapted control signal

Appendix D

Tuning parameters for the experiments

The following table presents the tuning parameters used in the experiments.

Table D.1: Tuning parameters for the boom function

Parameter	Value	Description
K_{fb}	$10 \cdot 10^{-3}$	Dynamic pressure feedback gain, higher value increase the impact from the pressure change
ω_n	2 Hz	The resonance frequency
ξ_1, δ_n	0.01	The width of the notch filter/damping of the system
ξ_2	1	The depth of the notch filter
ω_{cl}	3	The lower cut-off multiplier on the resonance frequency for the band-pass filter
ω_{cu}	1/3	The upper cut-off multiplier on the resonance frequency for the band-pass filter
ξ	$\sqrt{2}/2$	The damping ratio of the band-pass filter

Appendix E

External experiments on the boom function

These external test covers the case when the crane is exposed to a load. In Figure E.1 the crane is stepped up with load, and respectively down in Figure E.2. The resonance frequency is then lower to 1.5 Hz compared to 2 Hz, and is the compared in Figure E.3. The experiments of using the actual joystick instead of step signals can be seen in Figure E.4, and in Figure E.5, which will give the same behaviour as the step response Figures in Section 7.3, the only difference is that the pressure spikes will be lower. This is due to the slower command signal on the joystick, creating a more controlled behaviour of the crane and less oscillations.

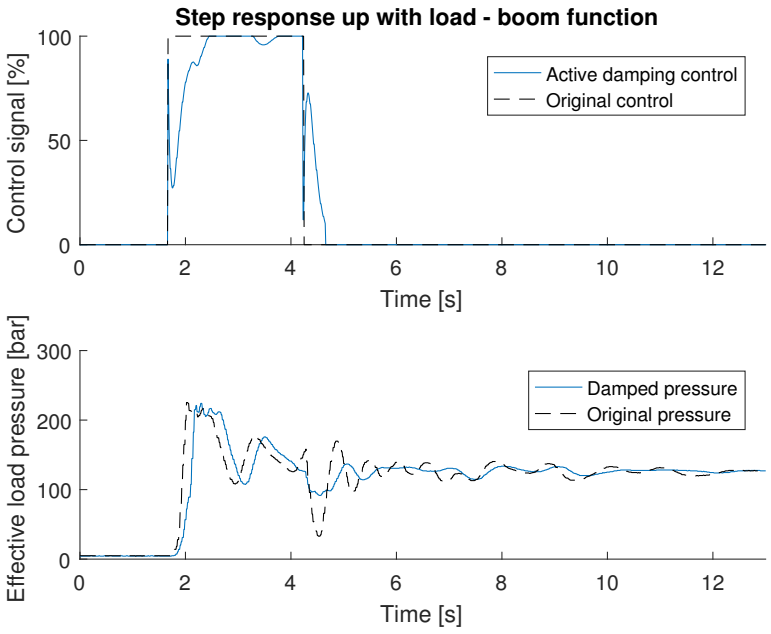

Figure E.1: Step response up of the boom function with load

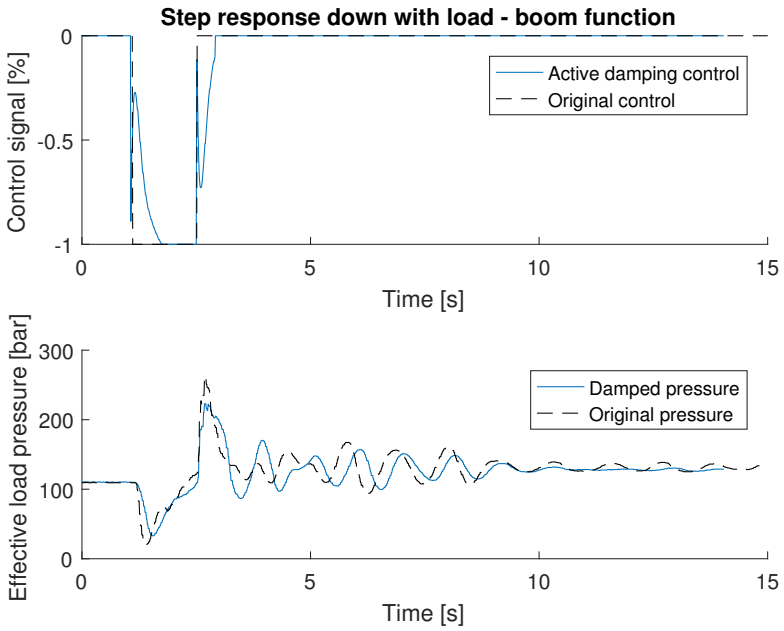

Figure E.2: Step response down of the boom function with load.

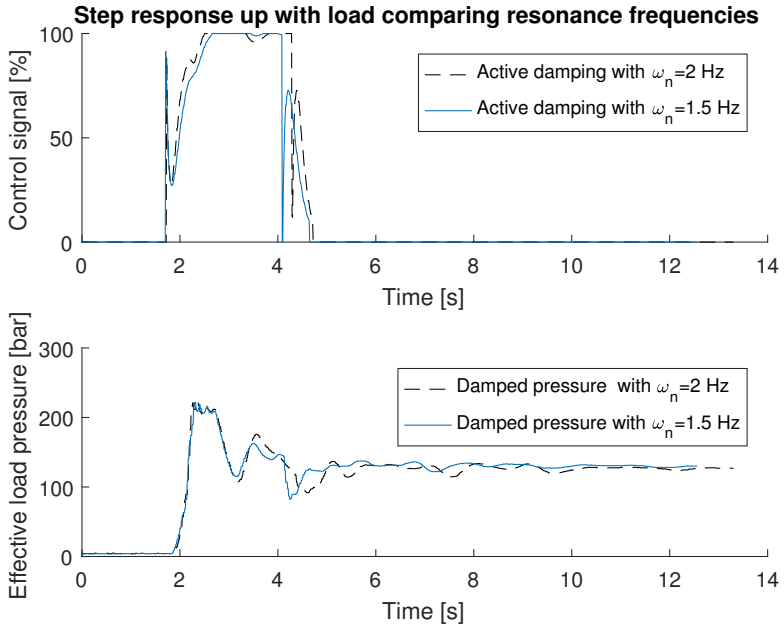

Figure E.3: Step response up of the boom function with load, comparing change of resonance frequency.

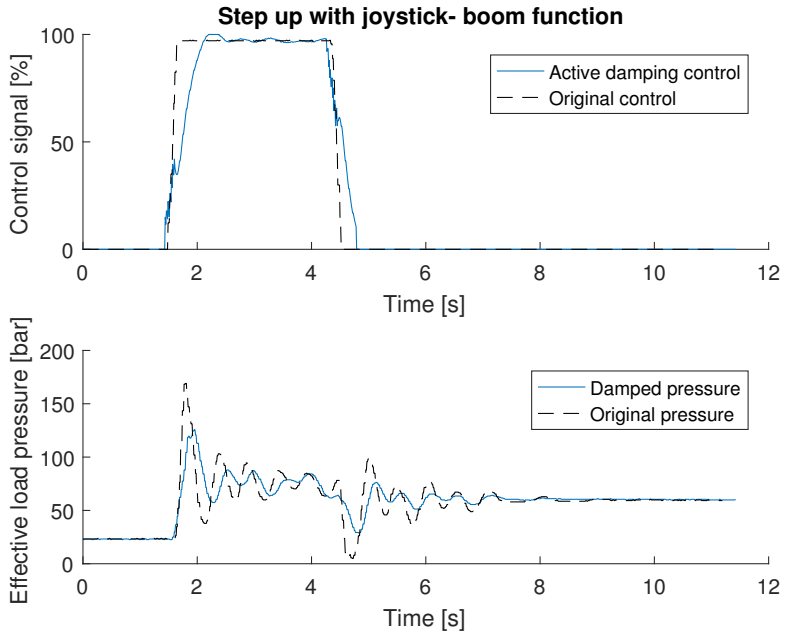

Figure E.4: Step up with joystick of the boom function.

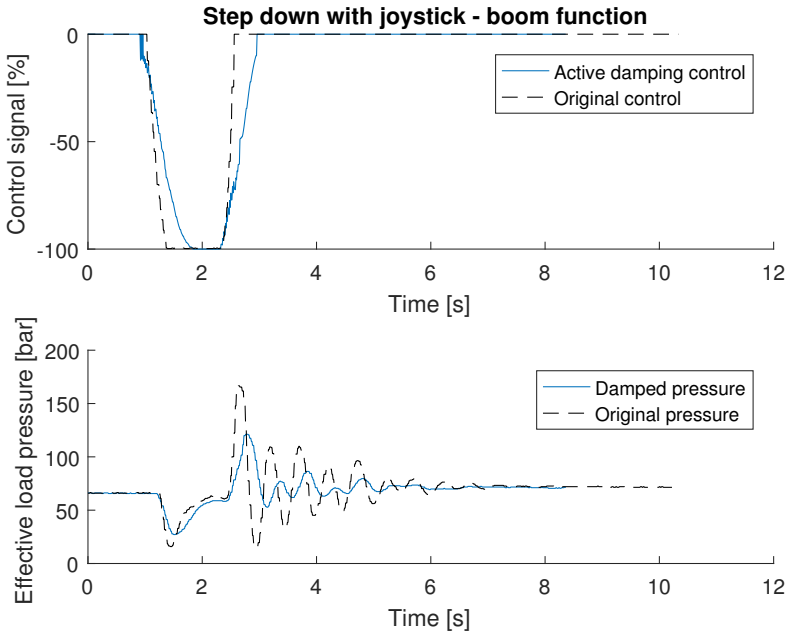

Figure E.5: Step down with joystick of the boom function.